Cell. Mol. Life Sci. (2017) 74:373–392
DOI 10.1007/s00018-016-2352-5

Cellular and Molecular Life Sciences

ORIGINAL ARTICLE

SUMOylation regulates the intracellular fate of ZO-2

Franziska Wetzel[1,6] · Sonnhild Mittag[1] · Misael Cano-Cortina[2] · Tobias Wagner[3] · Oliver H. Krämer[4] · Rainer Niedenthal[5] · Lorenza Gonzalez-Mariscal[2] · Otmar Huber[1]

Received: 24 February 2016 / Revised: 3 August 2016 / Accepted: 29 August 2016 / Published online: 7 September 2016

Abstract The zonula occludens (ZO)-2 protein links tight junctional transmembrane proteins to the actin cytoskeleton and associates with splicing and transcription factors in the nucleus. Multiple posttranslational modifications control the intracellular distribution of ZO-2. Here, we report that ZO-2 is a target of the SUMOylation machinery and provide evidence on how this modification may affect its cellular distribution and function. We show that ZO-2 associates with the E2 SUMO-conjugating enzyme Ubc9 and with SUMO-deconjugating proteases SENP1 and SENP3. In line with this, modification of ZO-2 by endogenous SUMO1 was detectable. Ubc9 fusion-directed SUMOylation confirmed SUMOylation of ZO-2 and was inhibited in the presence of SENP1 but not by an enzymatic-dead SENP1 protein. Moreover, lysine 730 in human ZO-2 was identified as a potential modification site. Mutation of this site to arginine resulted in prolonged nuclear localization of ZO-2 in nuclear recruitment assays. In contrast, a construct mimicking constitutive SUMOylation of ZO-2 (SUMO1ΔGG-ZO-2) was preferentially localized in the cytoplasm. Based on previous findings the differential localization of these ZO-2 constructs may affect glycogen-synthase-kinase-3β (GSK3β) activity and β-catenin/TCF-4-mediated transcription. In this context we observed that ZO-2 directly binds to GSK3β and SUMO1ΔGG-ZO-2 modulates its kinase activity. Moreover, we show that ZO-2 forms a complex with β-catenin. Wild-type ZO-2 and ZO-2-K730R inhibited transcriptional activity in reporter gene assays, whereas the cytosolic SUMO1ΔGG-ZO-2 did not. From these data we conclude that SUMOylation affects the intracellular localization of ZO-2 and its regulatory role on GSK3β and β-catenin signaling activity.

Keywords Tight junction · Zonula occludens-2 · β-Catenin · Glycogen-synthase-kinase-3β · Occludin

Abbreviations

GSK3β	Glycogen-synthase-kinase-3β
MDCK	Madin–Darby canine kidney
NES	Nuclear export signal
NLS	Nuclear localization signal
PLAs	Proximity ligation assays
SENP	Sentrin-specific protease
SUMO	Small ubiquitin-like modifier
TJ	Tight junction
UFDS	Ubc9 fusion-directed SUMOylation
ZO-2	Zonula occludens-2

Electronic supplementary material The online version of this article (doi:10.1007/s00018-016-2352-5) contains supplementary material, which is available to authorized users.

✉ Otmar Huber
otmar.huber@med.uni-jena.de

[1] Institute of Biochemistry II, Jena University Hospital, Friedrich-Schiller-University Jena, Nonnenplan 2-4, 07743 Jena, Germany

[2] Department of Physiology, Biophysics and Neuroscience, Center for Research and Advanced Studies (Cinvestav), Mexico City 07360, Mexico

[3] Institute of Biochemistry and Biophysics, Friedrich-Schiller-University Jena, CMB Center for Molecular Biomedicine, Hans-Knöll-Str. 2, 07745 Jena, Germany

[4] Department of Toxicology, University Medical Center Mainz, 55131 Mainz, Germany

[5] Institute of Physiological Chemistry/Biochemistry, Hannover Medical School, Carl-Neuberg-Str. 1, 30625 Hannover, Germany

[6] Present Address: Institut für Ernährungswissenschaften, Abt. Humanernährung, Dornburger Str. 29, 07743 Jena, Germany

Introduction

Tight junctions (TJs) represent the most apical cell–cell contacts of epithelial and endothelial cell layers. They regulate the paracellular passage of solutes and ions and maintain the polarized apical and basolateral distribution of proteins [1]. Besides these barrier and fence functions, TJs act as highly dynamic signaling platforms, which are integrated into numerous signaling pathways and regulate a variety of cellular processes involved in differentiation, proliferation and apoptosis [2]. Integral transmembrane proteins of the claudin family together with JAM proteins and the TJ-associated MARVEL protein (TAMP) family members occludin, tricellulin and MarvelD3 define the specific structure of the TJ strands between opposing cell surfaces and their barrier characteristics. At the cytoplasmic side of the TJ strands adaptor proteins including zonula occludens (ZO) proteins and cingulin link TJs to the actin cytoskeleton [3]. In addition, multiple proteins including kinases, phosphatases, small G-proteins and regulators of transcriptional processes [4] can be recruited to the cytosolic site of TJs thereby forming a signaling platform important for epithelial and endothelial homeostasis [2].

Zonula occludens-2 (ZO-2) was identified as a 160 kDa TJ-associated protein which is composed of multiple domains defining it as a MAGUK (membrane-associated guanylate kinase) protein family member [5]. In this respect, the amino-terminal part contains three PDZ-domains, followed by a central hinge region including a SH3-GuK (guanylate kinase) homologous module. The carboxy-terminal region includes acidic and proline-rich motifs that together constitute an actin-binding region (ABR) and ends with the PDZ-binding motif TEL. Along with its scaffold function different junction-associated proteins have been identified to bind to ZO-2 including occludin, claudins, connexin-36 and -43, JAM-A, ZO-1, α-catenin and others. Multiple further interaction partners binding to ZO-2 have been identified (for review see [6–8]) suggesting pleiotropic activities. In this context, mutations in ZO-2 causing amino acid exchange in the first PDZ domain or protein truncation resulted in disruption of hepatic TJs and development of familial hypercholanemia [9] and of progressive familial intrahepatic cholestasis [10], respectively, the latter revealing neurological and respiratory disorders in addition to the hepatic phenotype [11]. Moreover, two missense mutations in ZO-2 were reported to lead to autosomal non-syndromic hearing loss [12] and heterozygous duplication of the ZO-2 gene was associated with progressive non-syndromic deafness [13]. ZO-2 knock-out mice show early embryonic lethality shortly after implantation due to compromised cell proliferation and enhanced apoptosis [14]. Analysis of mouse chimera to rescue embryonic lethality revealed a critical role of ZO-2 for blood-testis barrier formation and male fertility [15].

Depending on the degree of cell–cell contacts formed, ZO-2 is a protein with dual localization. In confluent monolayers ZO-2 is predominantly associated with TJs, whereas in sparse cultures it is also located in the nucleus [16]. During recent years the ZO-2 nuclear function attracted much attention and a number of nuclear interaction partners were identified including transcription factors such as c-Jun, Fos, C/EBP [17], c-Myc [18], KyoT2 [19] thereby regulating transcription of genes such as cyclin D1 [18]. Further nuclear interaction partners include lamin B [20], the splicing factor SC35 [16] and SAF-B (scaffold attachment factor-B) [21]. Interestingly, ZO-2 appears to mediate the nuclear import of proteins including LASP-1 [22] and YAP2 [23], which acts as a transcriptional cofactor in the Hippo signaling pathway. Moreover, ZO-2 acts as a negative regulator of Wnt/β-catenin signaling [24, 25]. Therefore, it is of special interest to understand the mechanisms involved in the regulation of ZO-2 nuclear/cytosolic translocation.

In this respect, analysis of the primary sequence has revealed that canine ZO-2 (cZO-2) contains multiple nuclear localization sequences (NLSs) in the spacer region between PDZ1 and PDZ2 domains, including two bipartite NLSs, two monopartite basic NLSs, one of them overlapping with the first bipartite NLS and SR/RS-motifs rich in serine-arginine dipeptides [20]. In addition, four nuclear export sequences (NESs) were functionally characterized, two were mapped to PDZ2 and two to the GuK domain of cZO-2 [26]. Interestingly, Ser369 in NES-1 of cZO-2 has to be phosphorylated by protein kinase Cε (PKCε) to be active in protein export, whereas mutation to alanine impairs nuclear export [27]. According to our current understanding, activation of protein kinase B (PKB)/Akt, e.g. by epidermal growth factor (EGF) signaling, leads through activation of serine-arginine protein kinase 1 (SRPK1) to hyperphosphorylation and nuclear translocation of ZO-2. Within the nucleus phosphorylation of Ser369 by PKCε and O-GlcNAcylation of Ser257 trigger export of cZO-2 from the nucleus. In the cytosol the O-GlcNAc modification is removed and in the course of cell–cell contact maturation, Ser257 in cZO-2 is phosphorylated by PKCζ. Persistent O-GlcNAcylation induced by inhibition of the O-GlcNAc hydrolase with PUGNAc triggers proteasomal degradation [28]. Cellular localization of ZO-2 in proliferating cells is regulated by the cell cycle with ZO-2 entering the nucleus at the late G1 phase and departing during mitosis [25].

In addition to phosphorylation and O-GlcNAcylation, SUMOylation represents a reversible and highly dynamic posttranslational modification that has been reported to regulate nuclear/cytoplasmic localization of target proteins,

as well as their activity, stability and binding to interaction partners [29]. Four isoforms of SUMO (small ubiquitin-like modifier 1–4) are known. SUMO activation and ligation is mediated by a three-step enzymatic cascade, which involves an E1 SUMO-activating enzyme (SAE1/2) [30, 31], an E2 SUMO-conjugating enzyme (Ubc9) [32, 33] and E3 SUMO-ligases similar to ubiquitination. Thereby, SUMO is finally attached to lysine residues of its targets by an isopeptide bond with the C-terminal glycine residues of the SUMO-proteins. Interestingly, in contrast to ubiquitination, SUMO is synthesized as a pro-form that has to be processed prior to activation and conjugation. This step is mediated by SENP proteases, which also act as SUMO-deconjugating enzymes [34].

The only TJ protein that was reported to be modified by SUMOylation is claudin-2 affecting protein stability [35]. The presence of evolutionary conserved, potential SUMOylation sites within the ZO-2 protein prompted us to study if ZO-2 can become SUMOylated and how this affects the nuclear-cytoplasmic shuttling and signaling function of ZO-2.

Materials and methods

Cell culture

MDCKII and HEK-293 cells were cultured in MEM and DMEM (PAA Laboratories GmbH) with 10 % (v/v) FCS and 100 U/ml penicillin, 100 µg/ml streptomycin under standard cell culture conditions as described previously [36]. MDCK ZO-2 KD cells were kindly provided by Christina van Itallie (Laboratory of Tight Junction Structure and Function, NHLBI, National Institutes of Health) and cultured as previously described [37].

Antibodies

Monoclonal anti-FLAG M2, anti-maltose-binding protein (clone MBP-17) and polyclonal anti-FLAG antibodies were purchased from Sigma (Schnelldorf, Germany); anti-β-catenin (clone 14), anti-Ubc9, anti-Lamin, anti-GSK3β antibodies were from BD Transduction Laboratories™/BD Biosciences (Heidelberg, Germany); anti-myc (clone 9E10) was purified from hybridoma culture supernatant; anti-P5D4 antibody was kindly provided by Dr. K. Friedrich (Jena University Hospital); anti-GAPDH antibody was from Merck Millipore (Darmstadt, Germany); anti-GFP antibody from Clontech Laboratories, Inc. (CA, USA); anti-ZO-2 and anti-ZO-1 antibodies were from Invitrogen™ (Darmstadt, Germany); monoclonal anti-SUMO1 from Santa Cruz Biotechnology (Texas, USA) and polyclonal anti-SUMO1 antibody was included in the SUMOLink™-Kit (Active Motif, La Hulpe, Belgium). HRP-labeled goat anti-mouse and anti-rabbit antibodies were from Dianova (Hamburg, Germany), Alexa Fluor™ 488- and Alexa-Fluor™ 594-labeled antibodies were obtained from Molecular Probes (Life Technologies, Darmstadt, Germany).

Plasmids

The indicated plasmids were generated using standard procedures. Oligonucleotides used for PCR are summarized in Suppl. Table 1. Full-length human ZO-2 expression constructs were cloned by digestion of pFLAG-CMV2-hZO-2 (provided by Dr. Marius Sudol, Weis Center for Research, PA, USA; Department of Medicine, Mount Sinai School of Medicine, NY, USA) with *Kpn*I/*Xba*I and subcloned into *Kpn*I/*Xba*I sites of the p3xFLAG-CMV10 vector [23]. For ligation into the *Bam*HI sites of the pCS2 + , pCS2+-NLS, pCS2+FLAG, pGEX-4T1 and into the *Eco*RI site of the pCU [38] vector, full-length human ZO-2 was amplified by PCR using p3xFLAG-CMV10-ZO-2 as a template. FLAG-SENP1, FLAG-SENP1 MUT (R630L, K631M) and FLAG-SENP3 were obtained from Dr. Stefan Müller (Max Planck Institute of Biochemistry, Martinsried, Germany) [39]. pSG5-His-SUMO1-Q94P/T65R was obtained from Dr. M. Lienhard Schmitz (Institute of Biochemistry, Medical Faculty, Justus-Liebig-University Giessen, Germany) [40]. Full-length mouse Ubc9 cDNA was amplified by PCR from pCU and subcloned into the *Bam*HI sites of the pMAL-p2x (New England Biolabs, Frankfurt am Main, Germany) and pCS2+myc$_6$ vector. Single or multiple mutations of K117R, K730R, K759R and K992R in ZO-2, the mutation of Q89P in SUMO2/3 and K14R in Ubc9 were performed with the Change-IT™ Multiple Mutation Site Directed Mutagenesis Kit (USB Europe GmbH, Staufen, Germany). The human SUMO1-ZO-2 fusion proteins were generated by digestion with *Bam*HI and *Bgl*II. The deletion constructs ZO-2ΔC (aa 1–604) and ΔNZO-2 (aa 598–1190) were amplified by PCR and subcloned into the *Bam*HI sites of the pGEX-4T1 vector. SUMO1 and SUMO2/3 were amplified by PCR from pEGFP-C2-SUMO1 and pEGFP-C2-SUMO2/3 [38] and subcloned into the *Bam*HI site of the pCMV4-FLAG vector. The SUMO1ΔGG variant was amplified by PCR using pCMV4-FLAG-SUMO1 as template. The cDNA of GSK3β was kindly provided by Dr. M. Krohn (Max Planck Institute of Immunology, Freiburg, Germany) and after PCR amplification was digested with *Bgl*II and ligated into the *Bam*HI site of the pCS2+myc$_6$ and pQE60 vector. The pCS2+, pCS2+-myc$_6$ and pCS2+-NLS vectors were obtained from Dr. R. Rupp (Adolf Butenandt Institute, LMU München, Germany). pCS2+FLAG and the β-catenin expression plasmids

pCS2+-β-cat, pCS2+-β-cat-S33A-myc$_6$, pQE60-β-cat were described previously [41–43]. EGFP-occludin was generated as reported in [44]. The sequences of all constructs were verified by re-sequencing.

Transient transfections and reporter gene assays

MDCKII and HEK-293 cells (50–80 % confluent) were transiently transfected with polyethylenimine (PEI; Polysciences Inc., Hirschberg, Germany) using a DNA:PEI (1 mg/ml) ratio of 1:4. Reporter gene assays were performed as described previously [45]. Both cell lines were grown in 6- (1×10^6 cells/well) or 24- (2×10^5 cells/well) well plates and were transiently transfected with the indicated constructs and filled up with empty vector. Topflash/Fopflash (pGL3-OT/OF) plasmids were used as reporter constructs (provided by Dr. Bert Vogelstein, Johns Hopkins University, Baltimore, USA). Cells were harvested 24 h after transfection and luciferase activity was measured with a dual luciferase reporter gene assay system. Transfection efficiency was normalized by co-transfection of a constitutive-active Renilla luciferase vector (phRL-Null). Mean values of at least three independent transfection experiments are presented for all reporter gene assays.

UFDS-assays

For UFDS assays 1×10^6 HEK-293 cells were seeded in 6-well plates and 24 h later transfected with the indicated constructs as described above. Cells were lysed 48 h later in ice-cold modified RIPA buffer (50 mM Tris/HCl pH 8.0, 150 mM NaCl, 0.1 % (v/v) SDS, 1 % (v/v) NP-40, 0.5 % (w/v) sodiumdesoxycholate) supplemented with 20 mM *N*-ethylmaleimide (Thermo Scientific, Darmstadt, Germany) and subsequently analyzed by western blotting with the indicated antibodies.

Cell lysis, immunoprecipitation and Western blot analyses

For immunoprecipitation 1×10^6 HEK-293 cells/6-well were transiently transfected with the indicated constructs in different combinations. After 48 h cells were lysed for 20 min at 4 °C with ice-cold modified RIPA buffer (50 mM Tris/HCl pH 8.0, 150 mM NaCl, 0.1 % (v/v) SDS, 1 % (v/v) NP-40, 0.5 % (w/v) sodiumdesoxycholate) to investigate the interaction of ZO-2 and SENP1/3, or lysis buffer A (10 mM imidazole pH 6.8, 100 mM NaCl, 300 mM sucrose, 2 mM $MgCl_2$, 0.2 % (v/v) Triton X-100, 10 mM EDTA pH 8.0, 1 mM NaF, 1 mM Na_2MoO_4, 1 mM Na_3Vo_4) to analyze the interaction of ZO-2 and β-catenin/GSK3β. Both lysis buffers included Complete^{TM} protease inhibitor mix (Roche, Mannheim, Germany). Lysates were cleared by centrifugation (10 min, 20.800×*g*). For immunoprecipitation 2 µg of the appropriate antibody were pre-bound to Protein A-Sepharose^{TM} (GE Healthcare, Freiburg, Germany). Immunoprecipitation and Western blot analyses were performed as described previously [45] using the indicated antibodies (anti-MBP 1:4.000; anti-FLAG M2, 1:10.000; anti-myc (9E10), 1:4.000; anti-SUMO1, 1:4.000; anti-GST, 1:10.000; anti-ZO-2, 1 µg/ml; anti-Ubc9, 1:500; anti-GFP, 1:5.000; anti-Lamin, 1:2.000; anti-β-catenin, 0.5 µg/ml).

For precipitation of endogenous β-catenin/ZO-2 and GSK3β/ZO-2 complexes, confluent MDCK II cells were lysed in cold 20 mM Tris/HCl pH 7.4, 137 mM NaCl, 1 % (v/v) NP-40, 1 mM EDTA by scraping cells from the plate and subsequent passage through an insulin needle (5×). Lysates were cleared by centrifugation (10 min, 20.800×*g*). Anti-β-catenin antibody was pre-bound to Protein A-Sepharose^{TM} beads (GE Healthcare, Freiburg, Germany) and lysates were incubated with the beads for 16 h. After 3× washing with lysis buffer precipitated proteins were analyzed by western blotting with anti-ZO-2 antibody and chemoluminescence detection.

Pull-down assays

Proteins used for in vitro association assays were expressed in *E. coli* strains as glutathione-*S*-transferase (GST)- or maltose-binding protein (MBP)-fusion proteins. For the expression of MBP-Ubc9 in *E. coli* XL1-blue, 400 ml of LB-Amp medium containing 1 % (w/v) glucose were inoculated from an overnight culture, grown to an OD_{578} of 0.5–0.8 and induced with 1 mM IPTG at 37 °C for 1 h. *E. coli* BL21 DE3 cultures for the expression of GST-ZO-2 were grown to an OD_{578} of 0.6, pelleted by centrifugation (15 min, 4 °C, 4750×*g*) and resuspended in M9-minimal medium. After incubation for 1 h at 37 °C, expression of the fusion protein was induced with 1 mM IPTG at 17 °C for 16–18 h. GST-ΔNZO-2 was expressed in the *E. coli* strain BL21 DE3 Rosetta. Protein expression was induced at OD_{578} of 0.5–0.8 with 1 mM IPTG for 1 h at 37 °C. For lysis, bacteria were collected by centrifugation (15 min, 4 °C, 4750×*g*), washed in lysis buffer (100 mM NaCl, 40 mM Tris/HCl, pH 8.0 for MBP-Ubc9; PBS, 1 mM $MgCl_2$, 1 mM $CaCl_2$ for GST-fusion proteins) and after addition of Complete^{TM}-EDTA (Roche, Mannhein, Germany) cells were lysed on ice with an UltraSonic Processor UP100H (Hielscher, Germany), sonotrode MS7 (7 mm) for 3× 15 pulses (80 % intensity, Cycle 0.5). After centrifugation (30 min, 4 °C, 20.800×*g*) supernatants were loaded onto Bio-Rad Poly-Prep chromatography columns filled with 1 ml gel bed of GSH-agarose (Sigma, Schnelldorf, Germany) or amylose beads (New England Biolabs,

Frankfurt, Germany) equilibrated in the corresponding lysis buffer and purified as described previously [46]. After extensive washing bound GST and MBP proteins were eluted in 100 mM NaCl, 40 mM Tris/HCl, pH 8.0 containing 20 mM glutathione or 20 mM maltose, respectively. Protein containing fractions were combined and dialyzed against 50 mM NaCl, 20 mM Tris/HCl, pH 8.0. All steps were performed at 4 °C. For pull-down assays 2 µg of GST or GST-fusion proteins were incubated with 2 µg of MBP-fusion proteins in pull-down buffer (20 mM Tris/HCl, pH 8.5, 100 mM NaCl, 1 mM EDTA, 0.25 % (v/v) NP-40, 10 % (w/v) glycerol) for 20 min at 4 °C. Insoluble material was removed by centrifugation (10 min, 4 °C, 20.800×*g*). The supernatant was subsequently incubated with GSH-agarose beads in pull-down buffer for 1 h at 4 °C. After four washing steps in the same buffer, protein complexes were eluted with 2× SDS sample buffer and analyzed by Western blotting.

Nuclear-membrane-fractionation

MDCKII cells were transfected with FLAG-hZO-2 WT, FLAG-hZO-2 K730R or FLAG-SUMO-hZO-2 using Lipofectamine 2000 (Invitrogen, Carlsbad, CA, USA). The first 6 h the cells were left untouched to allow the proteins to be expressed, as recommended by the Lipofectamine 2000 manufacturer (time 0). Four or 24 h later, nuclear and membrane fractions were obtained using the Compartmental Protein Extraction Kit (2145RF, Millipore, Temecula, CA, USA) following the manufacturer's instructions. Nuclear and membrane fractions were subjected to an SDS-PAGE, and blotted with anti-FLAG antibody (F3165, dilution 1:5000, Sigma Aldrich, St Louis, MO, USA); lamin B1 (33-2000, dilution 1:500, Invitrogen, San Francisco, CA, USA), for identification of nuclear fractions; and anti-β1 subunit of Na^+/K^+-ATPase (kindly donated by Michael Caplan, Yale University, New Haven, CT, USA), for identification of plasma membrane fractions.

Nuclear recruitment assay

At different time points taken after transfecting MDCKII cells with $FLAG_3$-hZO-2 WT, $FLAG_3$-hZO-2 K730R or $FLAG_3$-SUMO-hZO-2, the cells were fixed and processed for immunofluorescence with an antibody against FLAG. The observations were initiated 6 h after transfection (time 0). In all experimental conditions, at each time point, the subcellular distribution patterns of $FLAG_3$-hZO-2 were analyzed in 100 transfected cells observed in an Eclipse E600 microscope (NIKON, Tokyo, Japan) using a 63× objective lens. The nuclear recruitment index refers to the percentage of transfected cells exhibiting nuclear stain and is integrated by cells displaying nuclear distribution in any of the following patterns: only nuclear, membrane and nuclear, cytoplasm and nuclear, and cytoplasm, nuclear and membrane, as previously described [27].

Detection of phosphorylated GSK3β in cell lysates

MDCKII monolayers were transfected using Lipofectamine 2000 (Invitrogen, Carlsbad, CA) with $FLAG_3$-hZO-2 WT, $FLAG_3$-hZO-2 K730R or $FLAG_3$-SUMO-hZO-2. After 24 h the cultures were lysed with modified RIPA buffer (50 mM Tris–HCl, pH 7.5, 150 mM NaCl, 1 % (v/v) NP-40), subjected to an SDS-PAGE, and blotted with antibodies against FLAG (F3165, dilution 1:5000, Sigma Aldrich, St Louis, MO, USA), anti p-GSK3β (Ser9) (5558P, dilution 1:1000, Cell Signaling, Danvers, MA, USA) and lamin B1 (33-2000, dilution 1:500, Invitrogen, San Francisco, CA, USA). The latter was used as loading control.

Duolink in situ proximity ligation assay

MDCKII cells (0.5×10^6 cells/well) were seeded on coverslips in 6-well plates. After 48 h, the cells were fixed with 2 % (w/v) paraformaldehyde in phosphate-buffered saline (PBS), pH 7.4, at 4 °C and permeabilized for 15 min with 0.5 % (v/v) Triton X-100 in PBS at room temperature. Olink Bioscience Duolink in situ proximity ligation assays (Sigma, Schnelldorf, Germany) were performed as described previously [47] using the indicated antibodies (anti-ZO-2, anti-FLAG polyclonal, anti-β-catenin, anti-GSK3β, anti-P5D4 1:300; anti-SUMO1 monoclonal, 1:100) for a 1 h incubation period. Images were taken with an inverse fluorescence microscope (Axio Observer with ApoTome, Zeiss, Germany) and quantified with Fiji open source software.

Results

ZO-2 is a potential target of SUMOylation

As a first step we analyzed the human ZO-2 amino acid sequence for potential SUMOylation sites using the SUMOsp 2.0 program (http://SUMOsp.biocuckoo.org/online.php) [48]. Six potential SUMOylation sites located in different ZO-2 domains were identified (Fig. 1a). Potential acceptor lysine residues within the domain structure of ZO-2 as well as nuclear export sequences (NES) and nuclear localization signals (NLS) are schematically presented in Fig. 1b. The high evolutionary conservation of sequence motifs containing the potential acceptor lysine residues is exemplified for the lysine residue 730 (K730) (Fig. 1c).

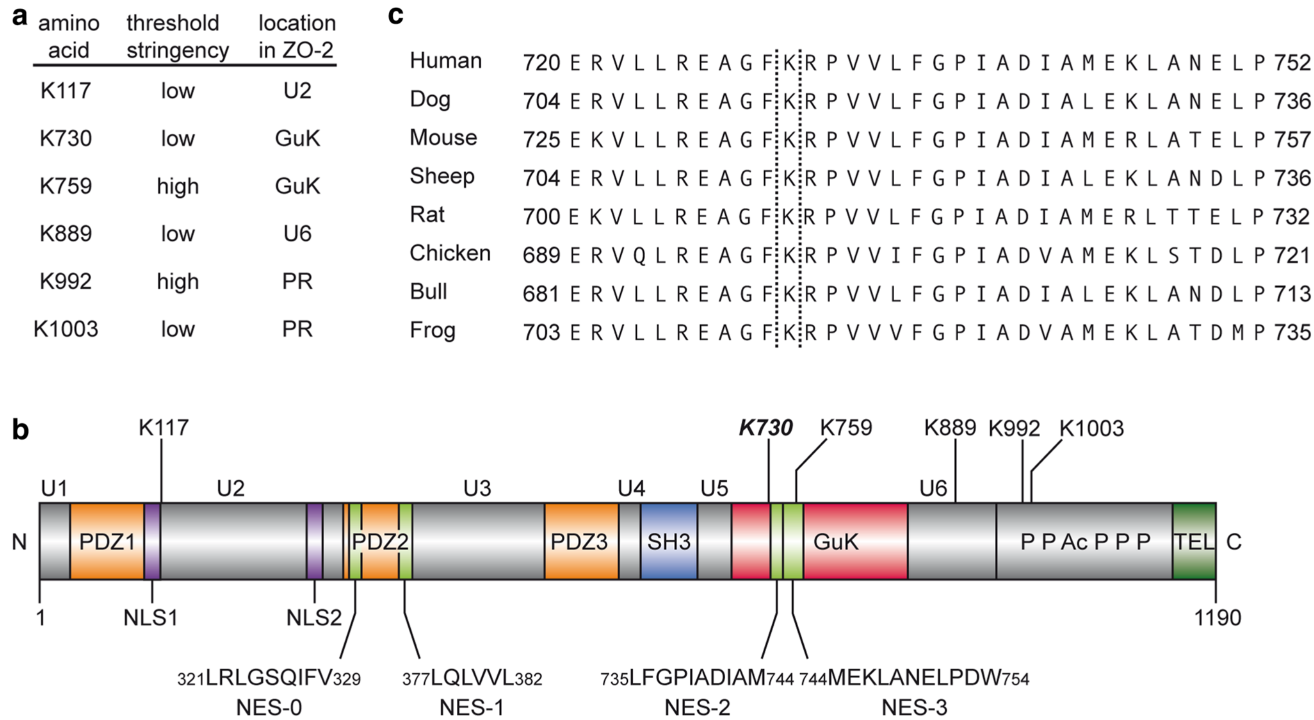

Fig. 1 ZO-2 is a potential target of SUMOylation. **a** Localization of potential SUMOylation sites in hZO-2 sequence employing low and high stringency thresholds with the SUMOsp 2.0 program (http://SUMOsp.biocuckoo.org/online.php). **b** Schematic representation of hZO-2 showing the localization of the potential SUMOylation sites. The four nuclear export sequences (NES) and two bipartite nuclear localization signals (NLS) in the region between PDZ- domains 1 (PDZ1) and 2 (PDZ2) are indicated. Lysine residues identified in **a** are marked with K followed by the specific amino acid number in human ZO-2. K730, which is of special interest in this study is marked in *bold*. *U1-6* linker regions, *GuK* guanylate kinase homologous domain, *PPAcPPP* proline-rich/acidic domain, *SH3* Src-homology 3 domain, *N* N-terminus, *C* C-terminus, *TEL* evolutionary conserved C-terminal amino acids threonine-glutamate-leucine. **c** K730 marked between the *dashed lines* is evolutionary conserved in ZO-2 as shown by the alignment of amino acid sequences from different species

Association of ZO-2 with Ubc9 and SENP1

If ZO-2 is a potential target for SUMOylation it has to be a substrate of components of the SUMOylation machinery. To test this we analyzed whether ZO-2 can form a complex with the E2 SUMO-conjugating enzyme Ubc9 in pull-down experiments. We used purified recombinant GST-ZO-2 and MBP-Ubc9 fusion proteins. A direct interaction of MBP-Ubc9 was detectable by Western blotting of protein complexes pulled down with GSH-agarose beads. No unspecific binding of MBP-Ubc9 to GST alone was detectable (Fig. 2a). Constructs encoding the N- or C-terminal part of ZO-2 also pulled-down MBP-Ubc9 revealing a preferential binding to the N-terminal part of ZO-2 (Online Resource 1).

In a further set of experiments, the association of ZO-2 with the SUMO-deconjugating proteases SENP1 and SENP3 was studied by co-immunoprecipitation experiments. HEK-293 cells were transiently transfected with pCS2+-ZO-2 and pCMV2-FLAG-SENP1 or pCMV2-FLAG-SENP3 and associated proteins were precipitated with anti-FLAG M2 antibody. Human ZO-2 was detectable in a complex with both SENP1 and SENP3 but not in precipitations from cell lysates transfected with one of these components alone (Fig. 2b).

Association of ZO-2 with two major components of the SUMOylation machinery further supported our hypothesis that ZO-2 is a target for SUMOylation.

ZO-2 is SUMOylated in cells and in vitro

SUMOylation is a highly dynamic and reversible post-translational modification, which is difficult to detect endogenously. To circumvent this problem we used the Ubc9 fusion-directed SUMOylation (UFDS) system [38]. In this assay Ubc9 is fused to the target protein of interest resulting in an enhanced SUMOylation. When HEK-293 cells were transiently transfected with a ZO-2-Ubc9 fusion construct together with EGFP-SUMO1 or -SUMO2/3 expression constructs a shifted band corresponding to SUMOylated ZO-2 was detectable in cell lysates by Western blotting with anti-Ubc9 antibody (Fig. 3a, b). Similar results were detectable when FLAG-tagged SUMO1 or SUMO2/3 constructs were used (Online Resource 2a, b). These band shifts clearly indicated a SUMOylation of the ZO-2-Ubc9 fusion protein. However,

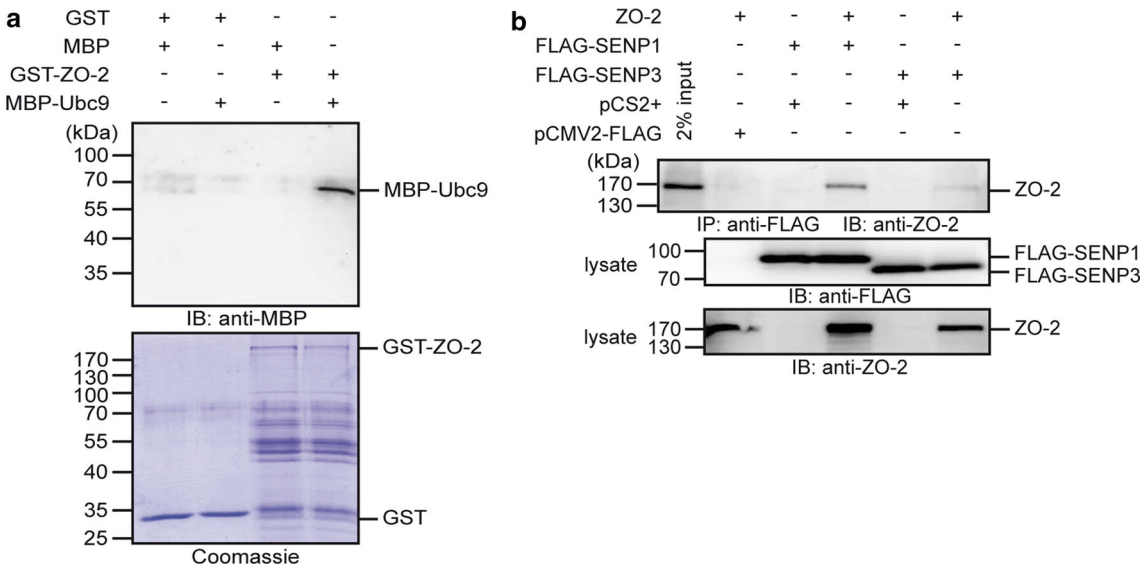

Fig. 2 ZO-2 specifically interacts with components of the SUMOylation machinery. **a** After incubation of purified recombinant GST (glutathione-*S*-transferase) or GST-ZO-2 with maltose-binding protein (MBP) or MBP-Ubc9 fusion proteins as indicated, protein complexes were pulled down with glutathione (GSH)-agarose, separated by SDS-PAGE and stained with Coomassie Blue or analyzed by Western blotting with an anti-MBP antibody. **b** HEK-293 cells were transiently transfected with different combinations of expression plasmids for ZO-2, FLAG-SENP1, FLAG-SENP3 or empty vectors pCS2+ or pCMV2-FLAG as controls. After lysis of cells immunoprecipitations were performed with the anti-FLAG M2 antibody and precipitates were subsequently analyzed by Western blotting with anti-ZO-2 antibody. Western blots of lysate controls are shown in the *lower panels*. Images are representatives of at least three independent experiments

when an Ubc9-ZO-2 construct with an N-terminal fusion of Ubc9 was transfected, no band-shift was observed (not shown). As Ubc9 can be auto-SUMOylated at lysine 14, we also tested a mutant ZO-2-Ubc9-K14R in the UFDS system [49]. Co-expression of EGFP-SUMO2/3 with ZO-2-Ubc9-K14R resulted in the same band-shift compared to co-expression with ZO-2-Ubc9 (Online Resource 2c). Thus, the auto-SUMOylation of Ubc9 is not responsible for the higher molecular weight band observed in the UFDS assays.

To further verify that the observed band-shift represents a SUMOylation-dependent modification of ZO-2, we used on the one hand a non-conjugatable SUMO1 construct missing the two C-terminal glycine residues necessary for covalent binding of SUMO to its substrate (FLAG-SUMO1ΔGG), and on the other hand a more protease-resistant SUMO2/3 variant (FLAG-SUMO2/3-Q89P) [50]. When ZO-2-Ubc9 was co-expressed with FLAG-SUMO1ΔGG no band-shift was visible (Fig. 3c). In contrast, co-expression of FLAG-SUMO2/3-Q89P resulted in a stronger band for ZO-2-Ubc9-FLAG-SUMO2/3 as observed before. In addition, a further super-shifted band became detectable (Fig. 3d) suggesting that multi- or poly-SUMOylation may occur.

Moreover, when we transfected HeLa cells with $FLAG_3$-ZO-2 and His_6-SUMO1-Q94P/T95R, another deSUMOylation-resistant form of SUMO1, and isolated SUMOylated proteins with Ni-NTA agarose beads, Western blot analyses with anti-FLAG M2 antibody detected a shifted $FLAG_3$-ZO-2 band which was visible with increased intensity after co-transfection of Ubc9 (Online Resource 3a). Further evidence that ZO-2 is a potential SUMOylation target was obtained when HA-tagged ZO-2 was immunoprecipitated from cell lysates and analyzed by Western blotting with an anti-SUMO1 antibody for modification with endogenous SUMO1 (Online Resource 3b).

Furthermore, the effect of co-expression of SENP1 on SUMOylation of ZO-2-Ubc9 in the UFDS assay was analyzed. The SUMOylation band-shift detectable in lysates of cells co-transfected with pCU-ZO-2-Ubc9 and pEGFP-C2-SUMO2/3 was significantly reduced by co-transfection of pCMV2-FLAG-SENP1-wt, but not when the catalytically inactive pCMV2-FLAG-SENP1-mut [51] was co-expressed (Fig. 3e, f).

In a next set of experiments, we applied proximity ligation assays (PLAs) to further investigate endogenous SUMOylation of ZO-2 in MDCKII cells. This assay is highly sensitive to detect endogenous protein complexes [52]. MDCKII cells were fixed and incubated with the polyclonal anti-ZO-2 and monoclonal anti-SUMO1 antibody for detection. Structured illumination microscopy images showed typical PLA signals for MDCKII cells, whereas in MDCKII ZO-2 knock-down cells used as a control, the number of dots was significantly decreased as

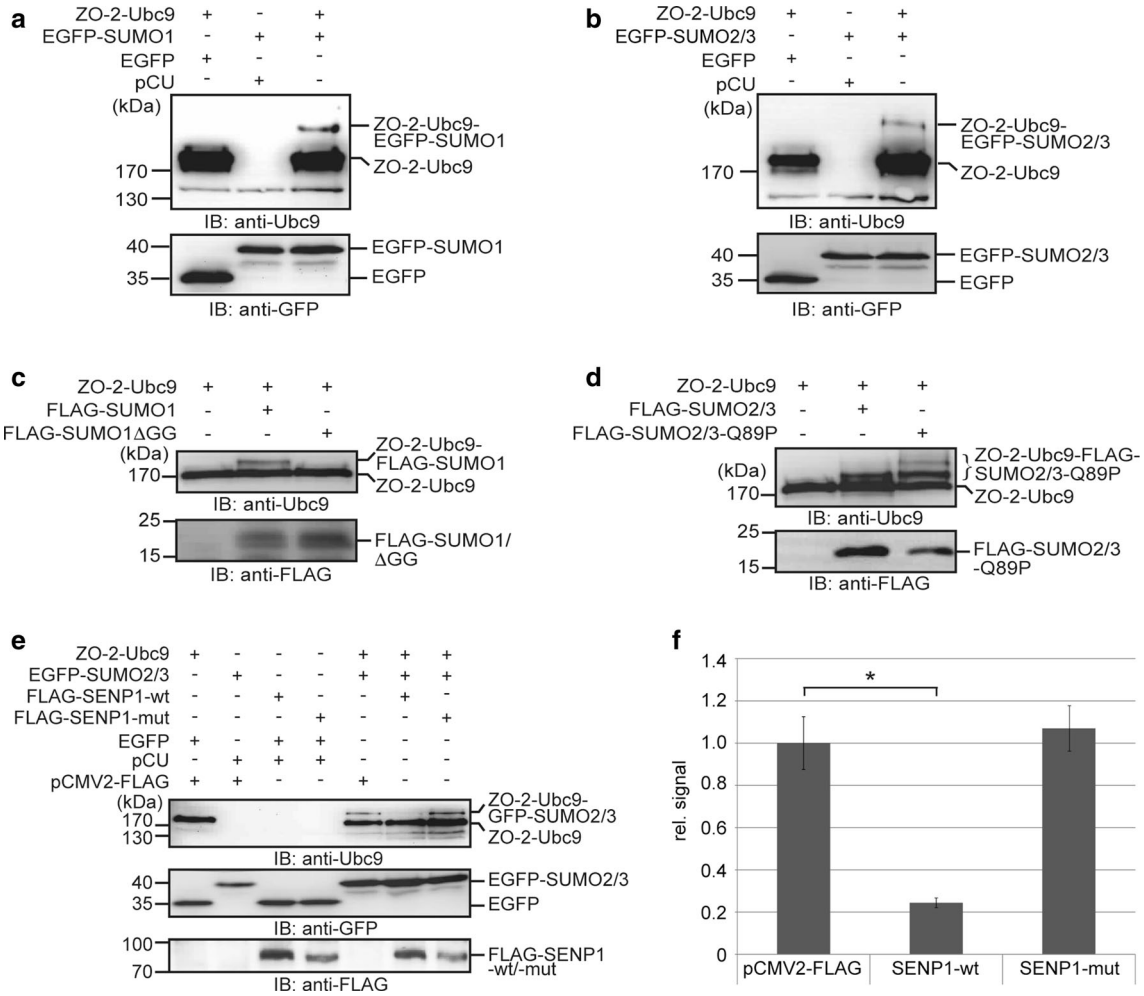

Fig. 3 Ubc9 fusion-directed SUMOylation (UFDS) defines ZO-2 as a SUMOylation target. UFDS assays were performed by transient transfection of HEK-293 cells with a ZO-2-Ubc9 fusion construct encoded in pCU and the indicated combinations of further expression vectors. Lysates were prepared 48 h after transfection and analyzed by Western blotting with the indicated antibodies. SUMOylation of the ZO-2-Ubc9 fusion construct resulting in a molecular mass shift of the fusion protein was detected by Western blotting with an anti-Ubc9 antibody. **a**, **b** Western blot analysis of HEK-293 cells transiently transfected with the ZO-2-Ubc9 fusion construct encoded in the vector pCU, and EGFP-tagged SUMO1 or SUMO2/3. Expression of comparable amounts of EGFP-SUMO fusion constructs was analyzed with an anti-GFP antibody as shown in the *lower panel*. EGFP and pCU represent empty vectors and were used as negative controls. **c** Co-expression of a FLAG-tagged SUMO1 construct with deletion of the C-terminal di-glycine motif (FLAG-SUMO1ΔGG) together with the ZO-2-Ubc9 fusion construct did not induce a SUMOylation-dependent band-shift compared to the wild-type construct FLAG-SUMO1. **d** Western blot analysis of lysates from HEK-293 co-expressing ZO-2-Ubc9 together with wild-type FLAG-SUMO2/3 or the de-SUMOylation-resistant FLAG-SUMO2/3-Q89P variant. Enhanced SUMOylation of the ZO-2-Ubc9 fusion construct is detectable as an additional shifted band. **e** Western blot analysis of HEK-293 cell lysates coexpressing ZO-2-Ubc9, EGFP-SUMO2/3 and the SUMO-deconjugating enzyme SENP1 (FLAG-SENP1-wt) or the proteolytically inactive SENP1 mutant (FLAG-SENP1-mut) as indicated. **f** Quantification of these experiments shows mean values ± SEM; $*p \leq 0.05$. At least three independent experiments were performed for all of the presented assays

well as in MDCKII cells incubated with secondary antibodies alone (Fig. 4). Most of the PLA signals representing SUMOylated ZO-2 were detectable in the cytosol suggesting that the majority of SUMOylated ZO-2 is localized in the cytosol.

Taken together these results provide good evidence that ZO-2 is modified by posttranslational SUMOylation.

K730 is an acceptor lysine for SUMOylation of ZO-2

Next, we wanted to identify the SUMOylation site in ZO-2. To this end we mutated 4 of the predicted potential acceptor lysines to arginine and examined them in the UFDS assay system. The fusion proteins ZO-2-K117R-Ubc9, -K730R, -K759R or -K992R were co-expressed with

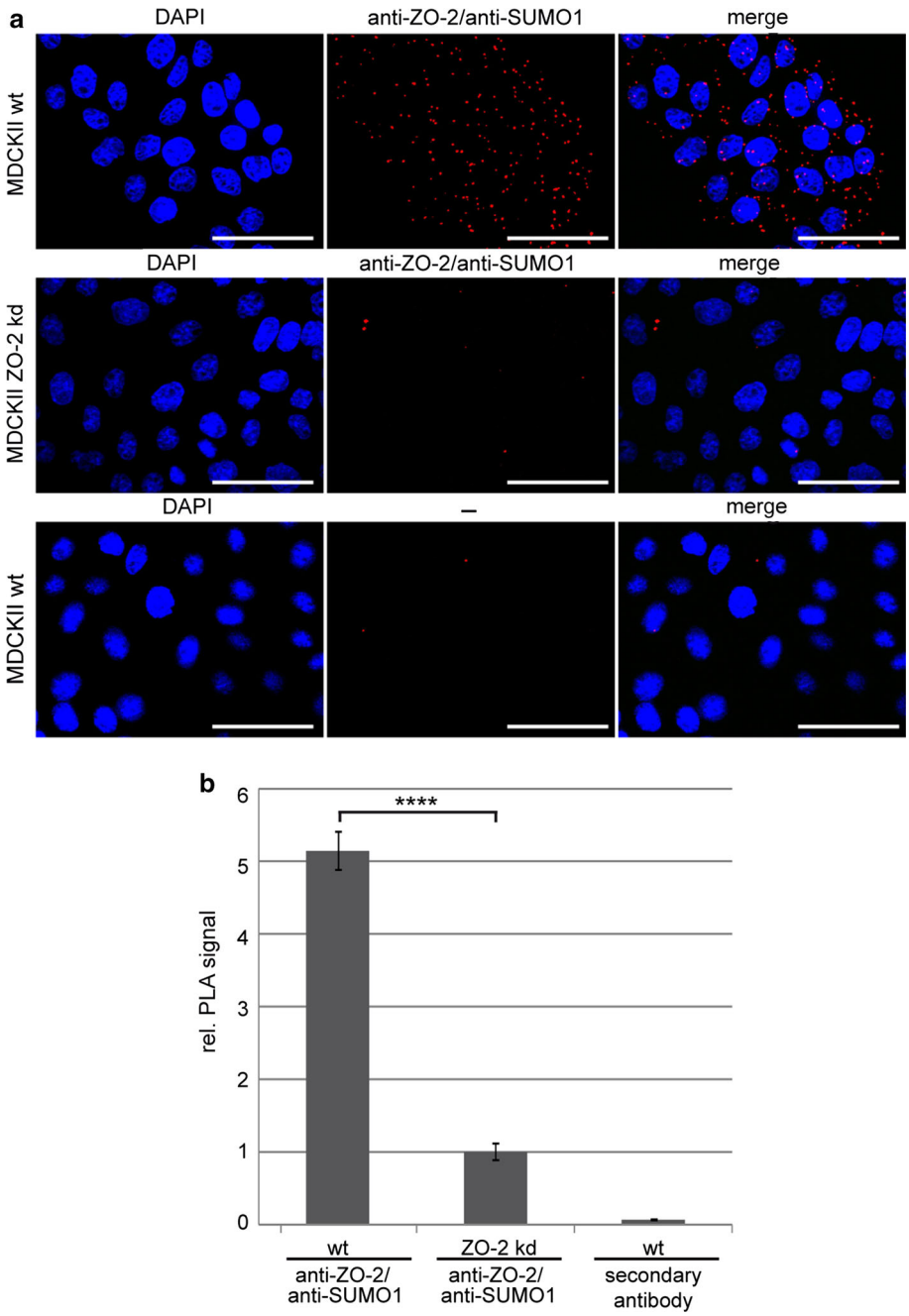

Fig. 4 ZO-2 is SUMOylated in the living cell. **a** MDCKII wild-type (wt) and MDCKII ZO-2 knock-down cells were analyzed by PLA using anti-ZO-2 and anti-SUMO1 antibodies or secondary antibody alone (–) as a control. PLA signals were detected by immunofluorescence microscopy. The images represent z-stack projections. **b** Quantification of PLA signals of three independent experiments using Fiji Software. PLA signals were related to cell numbers and values were normalized to MDCKII ZO-2 knock-down (kd) cells. Mean values ± SEM are presented and significances were analyzed by *t* test. $^{****}p \leq 0.0001$. *Scale bar* 50 µm

EGFP-SUMO2/3 and cell lysates were analyzed by SDS-PAGE and Western blot with anti-Ubc9 and anti-GFP antibodies. Signals for the SUMOylated ZO-2-Ubc9 were quantified in relation to the unmodified ZO-2-Ubc9 and normalized to ZO-2-wt-Ubc9. In this assay the SUMOylation of ZO-2-K730R-Ubc9 was significantly reduced (Fig. 5a).

To further support that lysine 730 is a potential acceptor lysine for SUMOylation in ZO-2, PLA assays were performed with HEK-293 cells 24 h after transient transfection with p3xFLAG-CMV-10-ZO-2-wt or p3xFLAG-CMV-10-ZO-2-K730R. Typical PLA signals were detectable in structured illumination microscopy images with ZO-2-wt and clearly reduced numbers with mutant ZO-2-K730R (Fig. 5b).

These experiments suggest that K730 in ZO-2 acts as a SUMO-acceptor site but further SUMOylation sites in ZO-2 cannot be excluded.

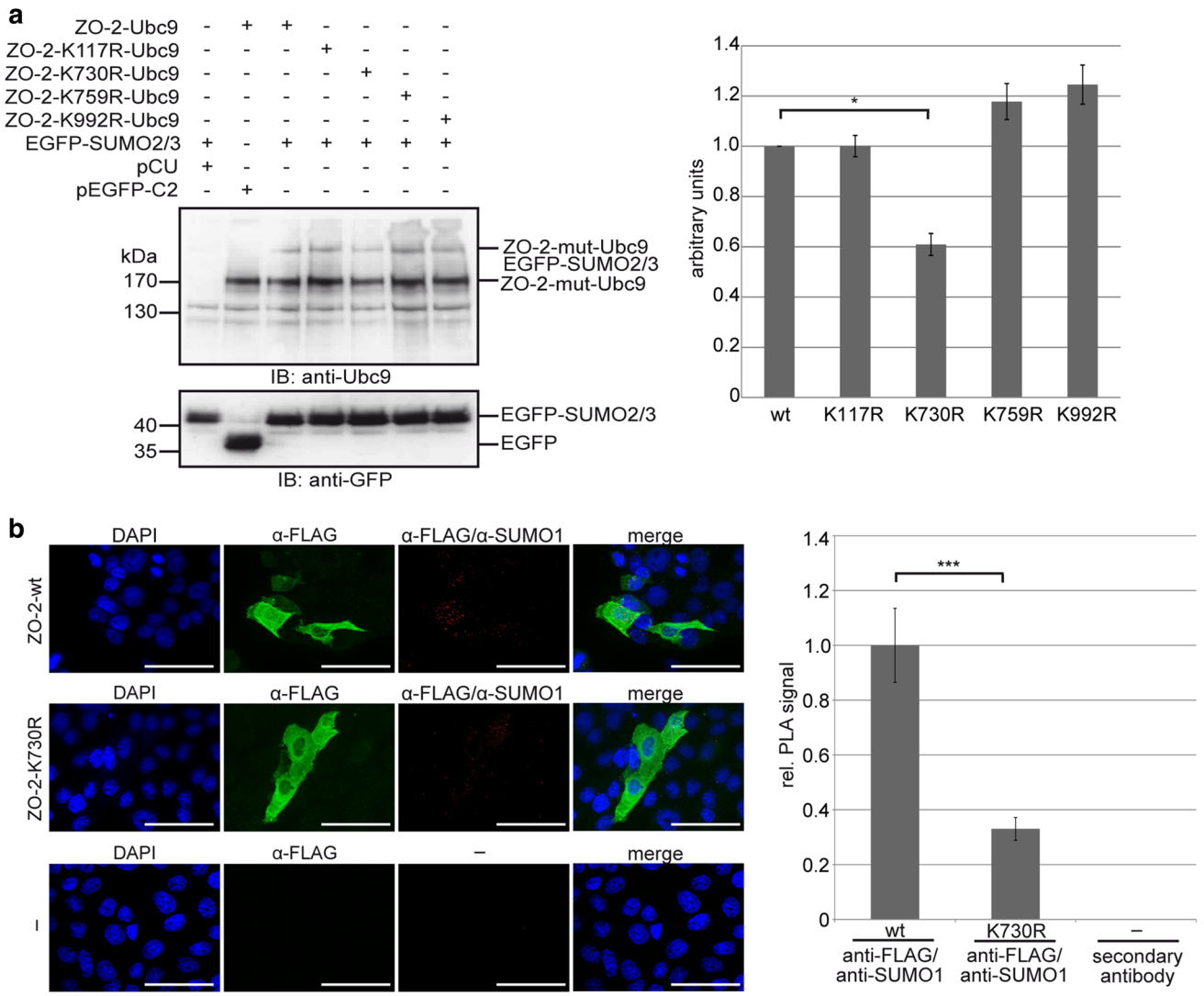

Fig. 5 Lysine 730 in ZO-2 is SUMOylated. **a** Wild-type ZO-2-Ubc9 was compared in UFDS assays with ZO-2-Ubc9 constructs mutated to arginine (R) at potential SUMOylation sites K117, K730, K759 and K992 as predicted by the SUMOsp 2.0 program. HEK-293 cells were transiently transfected with the indicated ZO-2-Ubc9 fusion constructs together with EGFP-SUMO2/3. Cell lysates were analyzed by Western blotting with an anti-Ubc9 antibody and anti-GFP antibody as a loading control. The *right panel* shows quantification of 6 independent experiments with mean values ± SEM. The wild-type construct was set to 1 and the mutated ZO-2 constructs are depicted relative to wild-type ZO-2. *$p \leq 0.05$. **b** SUMOylation of ZO-2-K730R is no longer detectable in PLAs. HEK-293 cells were transiently transfected with p3xFLAG-CMV-10-ZO-2-wt or p3xFLAG-CMV-10-ZO-2-K730R and analyzed 24 h later with anti-FLAG and anti-SUMO1 antibody. To detect transfected cells, the monolayer was treated with Alexa Flour® 488-labelled secondary antibody. The confocal images correspond to z-stack projections. The *right panel* shows quantification of PLA signals relative to the area of transfected cells and normalized to the FLAG-tagged ZO-2-wt control. Mean values ± SEM and significances analyzed by *t* test (***$p \leq 0.001$) are presented. *Scale bar* 50 µm

SUMOylation affects cellular ZO-2 localization

Protein localization is often affected by SUMOylation [53] and therefore, we wondered if this is also valid in respect to nuclear/cytosolic distribution of ZO-2. Since the very limited amounts of SUMOylated endogenous protein impede evaluation of the functional consequences of the modification, constitutive SUMOylation can be mimicked by addition of SUMO to the N- or C-terminal ends of the target protein of interest [54, 55].

To generate a ZO-2 variant mimicking constitutive SUMOylation of ZO-2, we attached a SENP-resistant $FLAG_3$-tagged SUMO1ΔGG moiety to the N-terminus of ZO-2. Immunoprecipitation experiments revealed that $FLAG_3$-SUMO1ΔGG-ZO-2 is not impaired in binding to occludin suggesting that important structural determinants at the N-terminus of ZO-2 remain intact (Online Resource 4a). These $FLAG_3$-SUMO1ΔGG-ZO-2, $FLAG_3$-ZO-2-wt or $FLAG_3$-ZO-2-K730R constructs were transiently transfected into MDCKII cells and subjected to nuclear/

membrane fractionation and subsequently analyzed by SDS-PAGE and Western blotting. At the time point 4 h (10 h after transfection) wild-type ZO-2 first accumulates in the nucleus and is then released into the cytosol where it reaches a junctional localization after 24 h. In contrast the K730R-mutated ZO-2 exhibited a strongly delayed nuclear export, whereas the constitutively SUMOylated ZO-2 cannot enter the nucleus (Fig. 6a).

In a next step we wanted to further confirm this difference in distribution in nuclear recruitment assays. FLAG-ZO-2-wt accumulated in the nucleus early after transfection but then started to leave the nucleus 4 h after transfection. Again, the SUMOylation-mutant ZO-2-K730R behaves different compared to wild-type ZO-2. About 55–65 % of the $FLAG_3$-ZO-2-K730R-transfected cells had ZO-2 in the nucleus for the analyzed time period. In contrast, only in 15–20 % of the $FLAG_3$-SUMO1ΔGG-ZO-2-transfected cells SUMOylation was detected in the nucleus (Fig. 6b). Corresponding immunofluorescence images are shown in Online Resource 4b.

From these results we conclude that SUMOylation induces a change in the intracellular distribution of ZO-2 resulting in a predominant cytosolic localization.

ZO-2 interacts with GSK3β

Our previous studies provided evidence that ZO-2 can reduce Ser9 phosphorylation of glycogen-synthase-kinase-3β (GSK3β) [25] resulting in activation of its kinase function. In the context of this study we wanted to address whether ZO-2 binds to GSK3β and if the SUMOylation of ZO-2 has an effect on Ser9 phosphorylation of GSK3β. Indeed, in HEK-293 cell lysates overexpressing $FLAG_3$-ZO-2 and GSK3β-myc_6 proteins, immunoprecipitation of myc_6-tagged GSK3β co-precipitated FLAG-tagged ZO-2 from lysates co-transfected with both construct but not when transfected with only one of them (Fig. 7a). Mutant ZO-2-K730R was not impaired in binding to GSK3β (Online Resource 5a). In addition, in immunoprecipitates of endogenous ZO-2 from MDCK cell lysates, GSK3β was detectable by Western blotting (Fig. 7b). Pull-down assays with purified recombinant proteins, GST-ZO-2 fusion proteins revealed a direct binding of GSK3β-His_6 preferentially to the ZO-2 N-terminal part (Online Resource 5b). In addition, PLAs performed with MDCKII cells supported endogenous complex formation of both proteins. PLA signals were clearly visible in MDCKII cells using anti-GSK3β with anti-ZO-2 antibodies but only at background levels when anti-ZO-2 was applied together with anti-P5D4 antibody as non-target control or in controls using secondary antibody alone (Fig. 7c). When we analyzed GSK3β-Ser9 phosphorylation levels in MDCKII cells transiently transfected with the FLAG-tagged wild-type ZO-2, its mutant ZO-2-K730R or the SUMO1ΔGG-fusion constructs, we observed that a reduced Ser9-phosphorylation was detectable for the SUMO1ΔGG-fusion construct compared to wild-type or K730R-mutated ZO-2 (Fig. 7d). Biochemical fractionation of cells into nuclear and cytoplasmic fractions illustrated that the cytoplasmic but not the nuclear fraction of ZO-2 decreased GSK3β-Ser9 phosphorylation (Online Resource 5c). These observations hence suggest that ZO-2 by interacting with GSK3β modulates GSK3β signaling function. The predominantly cytosolic localization of the SUMO1ΔGG-ZO-2 fusion construct appears to enhance this effect.

SUMOylation of ZO-2 affects β-catenin/TCF-4 signaling

In a previous study we have shown that ZO-2 acts as a repressor of β-catenin/TCF-4 signaling [25]. The observation that SUMOylation alters the localization of ZO-2 suggested that this also might affect its repressive effect on β-catenin/TCF-4-mediated transcriptional activity. To this end Topflash/Fopflash reporter gene assays were performed in HEK-293 cells.

Transfection of β-catenin together with TCF-4 resulted in an increased activation of transcriptional activity. As observed previously, co-transfected $FLAG_3$-ZO-2-wt acted as a repressor. However, this repressive activity was not detectable for the constitutively SUMOylated $FLAG_3$-SUMO1ΔGG-ZO-2 construct (Fig. 8a). Similar effects were obtained for a Siamois-luciferase construct containing the promoter of an endogenous Wnt target gene (Fig. 8b). A N- or C-terminal position of the FLAG-tag did not affect the results (compare with Online Resource 6a). Moreover, when we tested the SUMOylation-mutant $FLAG_3$-ZO-2-K730R a minor but significant increase in the repressive activity was detectable (Online Resource 6b).

From these experiments we concluded that SUMOylation of ZO-2 reduces the repressive activity on β-catenin transcriptional activity and the nuclear fraction of ZO-2 mediates the repressive effect. Therefore, a ZO-2 construct with a C-terminally fused NLS should have an even stronger repressive effect. The ZO-2-NLS construct revealed nuclear localization even in dense culture (Online Resource 6c) and thus appears to overrule endogenous NLS/NES signals. It completely inhibited Topflash activity confirming our assumption (Fig. 8c). A similar effect was observed in Siamois Reporter gene assays (Online Resource 6d).

In a next step we wanted to address if this nuclear function of ZO-2 is mediated directly by β-catenin or if ZO-2 indirectly affects β-catenin-LEF-1/TCF transcriptional activity. To test this we made use of the ΔNLEF-1-VP16 construct, which has a deleted N-terminal β-catenin

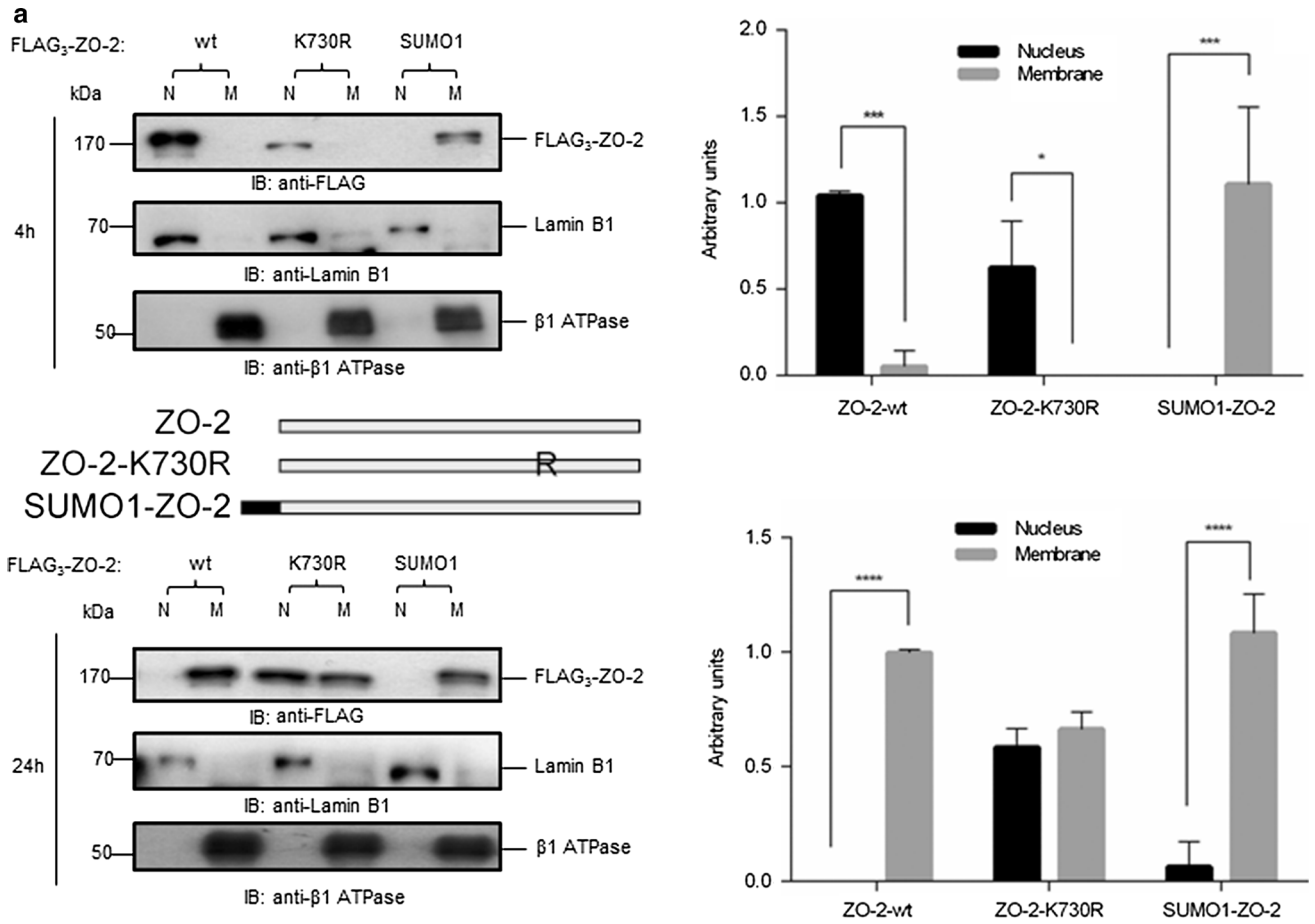
a
FLAG3-ZO-2: wt K730R SUMO1
kDa N M N M N M
170
FLAG3-ZO-2
IB: anti-FLAG
4h
70
Lamin B1
IB: anti-Lamin B1
50
β1 ATPase
IB: anti-β1 ATPase
ZO-2
ZO-2-K730R
R
SUMO1-ZO-2
FLAG3-ZO-2: wt K730R SUMO1
kDa N M N M N M
170
FLAG3-ZO-2
IB: anti-FLAG
24h
70
Lamin B1
IB: anti-Lamin B1
50
β1 ATPase
IB: anti-β1 ATPase
Nucleus
Membrane
Arbitrary units
2.0
1.5
1.0
0.5
0.0
***
*
***
ZO-2-wt
ZO-2-K730R
SUMO1-ZO-2
Nucleus
Membrane
Arbitrary units
1.5
1.0
0.5
0.0
****
****
****
ZO-2-wt
ZO-2-K730R
SUMO1-ZO-2

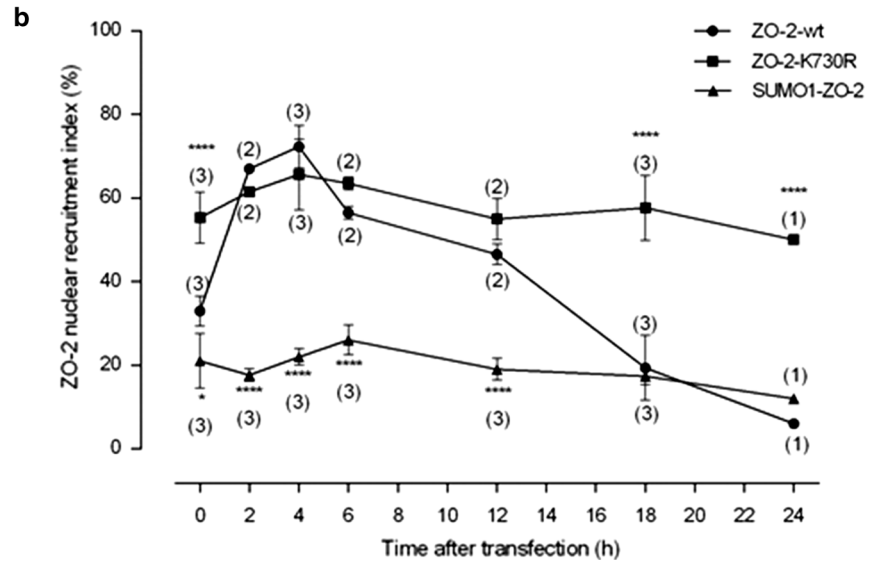
b
ZO-2-wt
ZO-2-K730R
SUMO1-ZO-2
ZO-2 nuclear recruitment index (%)
100
80
60
40
20
0
0 2 4 6 8 10 12 14 16 18 20 22 24
Time after transfection (h)

◀**Fig. 6** SUMOylation of ZO-2 affects its intracellular localization. MDCK cells were transiently transfected with empty vector p3xFLAG-CMV10 (pCMV10), $FLAG_3$-ZO-2-wt (ZO-2), $FLAG_3$-ZO-2-K730R (ZO-2-K730R) or $FLAG_3$-SUMO1ΔGG-ZO-2 (SUMO1-ZO-2) and subjected to a nuclear recruitment assay or to nuclear/membrane fractionation 4 and 24 h after transfection considering that $t = 0$ h starts after the initial 6 h post transfection needed for de novo protein expression. **a** Cells were lysed at the indicated time points, and nuclear/membrane fractions were subsequently analyzed by SDS-PAGE and Western blotting with anti-FLAG antibody. As controls, anti-lamin A/C and anti-β1-ATPase antibodies were used. The presented blot is a representative of three independent experiments. **b** Nuclear recruitment assay. Cells were seeded at a density of 1.9×10^5 cells/cm^2 and were fixed and processed for immunofluorescence microscopy at the indicated time points after transfection (see *above*) using an anti-FLAG antibody and the percentage of cells with nuclear ZO-2 was determined. The number of independent experiments is indicated in *parentheses*. In each experiment the distribution pattern for transfected ZO-2 was analyzed in 100 cells for each time point. ****$p \leq 0.0001$, using a Bonferroni's multiple comparisons test comparing experimental to control values

binding-site and is C-terminally fused to the Herpes virus VP16 transactivation domain which mediates transcriptional activation independent of β-catenin [56]. HEK-293 cells were co-transfected with this construct and wild-type ZO-2 or ZO-2-NLS and Top/Fopflash reporter gene assays were performed. Both constructs inhibited the reporter gene activity in a β-catenin-independent manner (Fig. 8d). Again similar results were obtained in Siamois reporter gene assays (Online Resource 6e). From these data we conclude, that the repressive effect of ZO-2 on β-catenin-LEF/TCF-mediated transcription is indirect and involves additional factors that have to be identified in future experiments.

Although ZO-2 apparently does not directly repress β-catenin-mediated transcription it cannot be excluded that both proteins form a complex. To address this point co-immunoprecipitation experiments were performed with lysates of transiently transfected HEK-293 cells revealing that FLAG-ZO-2 and β-catenin-S33A-myc_6, a stabilized variant of β-catenin, form a common complex (Fig. 9a). Moreover, we could detect endogenous ZO-2/β-catenin complexes in immunoprecipitations with an anti-β-catenin antibody (Fig. 9b). PLAs in MDCKII cells confirmed close proximity and showed an accumulation of PLA signals at sites of or close to cell–cell contacts. Only a minor number of signals were detectable in MDCKII ZO-2 knock-down cells or in control experiments performed only with the secondary antibody (Fig. 9c, d). A similar distribution of PLA signals was detectable for ZO-1 and β-catenin which have been reported to form a complex [57] (Online Resource 7). Pull-down assays using recombinant GST-ZO-2 constructs encoding the N- or C-terminal part of ZO-2 and β-catenin-His_6 indicated that the interaction between ZO-2 and β-catenin is direct and suggested that binding-sites in both constructs exist (Online Resource 8a). The association of ZO-2-K730R to β-catenin is not affected (Online Resource 8b). Taken together, our data imply that ZO-2 in directly interacting with β-catenin and GSK3β modulates its dual function in adhesion and signaling.

Discussion

Changes in physiological and pathological conditions, and activation of signaling pathways often are associated with altered intracellular localization of proteins thereby allowing access to interaction partners present at specific sites or compartments of a cell. During recent years, a number of proteins with dual localization either at sites of cell–cell contacts or in the nucleus [2, 58] have been identified. These factors exhibit distinct functions affecting multiple processes including proliferation, apoptosis, differentiation and morphogenesis. For example, ZO-2 on the one hand acts in association with JAM-A, occludin and claudins as a multifunctional scaffold linking TJs to the actin cytoskeleton and as an adaptor for TJ-associated proteins. On the other hand, in proliferating or stressed cells ZO-2 is located in the nucleus in a cell cycle-dependent manner [25] where it interacts with nuclear factors and thereby regulates gene transcription, splicing, cell proliferation, etc. [8]. In this context the localization of ZO-2 has to be tightly regulated.

Given that SUMO modifications affect nuclear/cytoplasmic transport of proteins [59] and that evolutionary highly conserved putative SUMOylation sites are present in ZO-2, we report in this manuscript that SUMOylation represents another modification involved in the regulation of ZO-2 localization and signaling function. Since the SUMOylation machinery only uses a single E2 conjugating enzyme, Ubc9, that often is directly involved in the selection of SUMOylation targets [33], the direct interaction of Ubc9 and ZO-2 in pull-down assays provided first evidence that ZO-2 is a SUMOylation target. The E3 SUMO-ligase involved in ZO-2 modification currently is unknown. For a coordinated regulation of the highly dynamic SUMO modification, in addition to SUMO conjugation, deconjugation is a further important step. According to this requirement, we observed a complex formation of ZO-2 with the SUMO-proteases SENP1 and SENP3. SENP1 is mainly localized in the nucleoplasm, whereas SENP3 appears to be enriched in the nucleolus [60]. This preferential localization suggested that ZO-2 is preferentially de-SUMOylated in the nucleus. To our knowledge a specific nucleolar function of ZO-2 has not been defined and thus it is not surprising, that only a weak signal for SENP3 was obtained in the co-immunoprecipitation experiments.

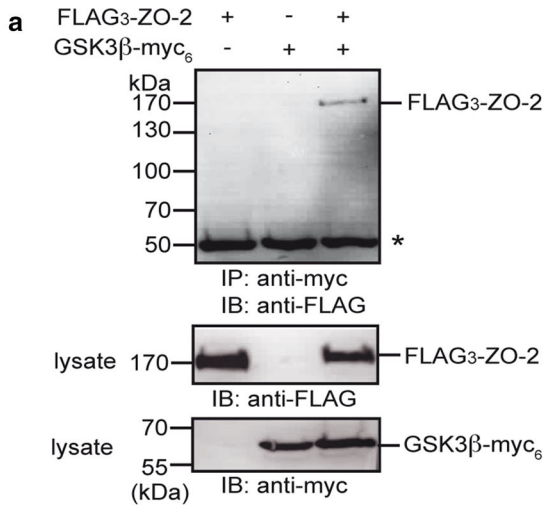
a
FLAG3-ZO-2 + - +
GSK3β-myc6 - + +
kDa
170
130
100
70
50
FLAG3-ZO-2
*
IP: anti-myc
IB: anti-FLAG
lysate 170
FLAG3-ZO-2
IB: anti-FLAG
lysate 70
55
(kDa)
GSK3β-myc6
IB: anti-myc

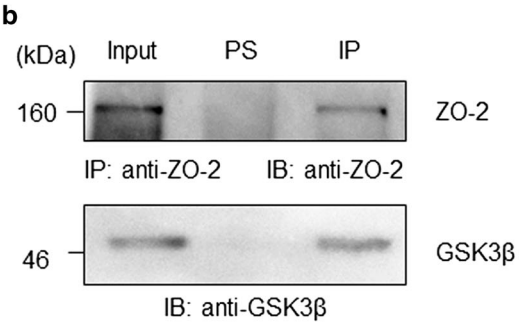
b
(kDa)
Input
PS
IP
160
ZO-2
IP: anti-ZO-2
IB: anti-ZO-2
46
GSK3β
IB: anti-GSK3β

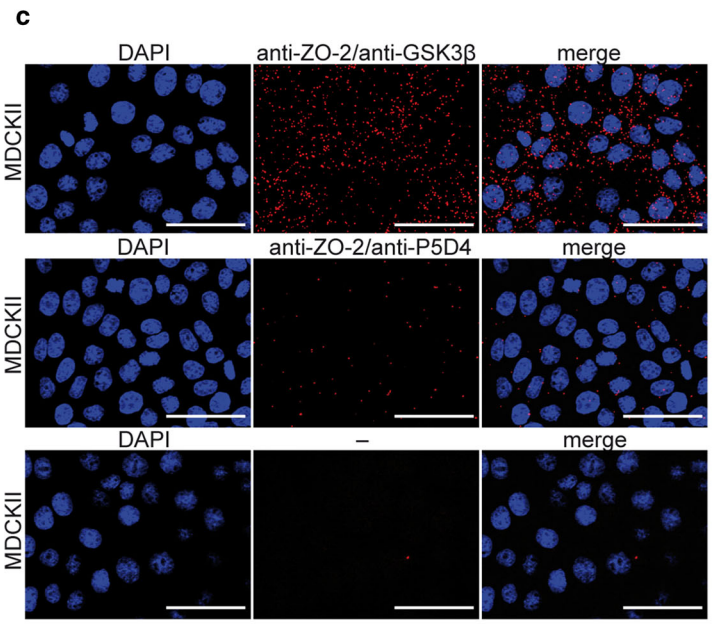
c
DAPI
anti-ZO-2/anti-GSK3β
merge
MDCKII
DAPI
anti-ZO-2/anti-P5D4
merge
MDCKII
DAPI
–
merge
MDCKII

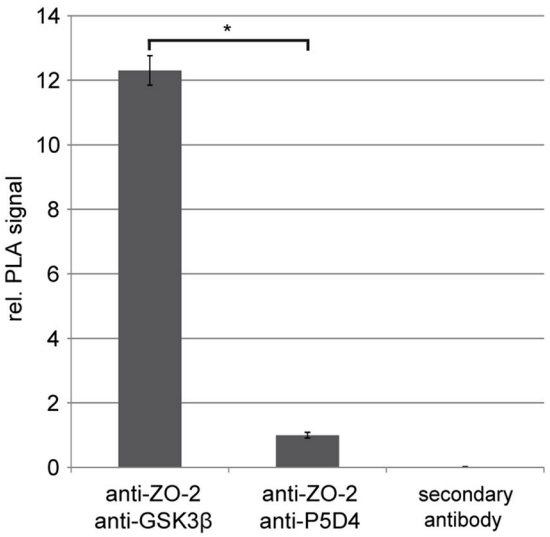
14
12
10
8
6
4
2
0
*
rel. PLA signal
anti-ZO-2
anti-GSK3β
anti-ZO-2
anti-P5D4
secondary
antibody

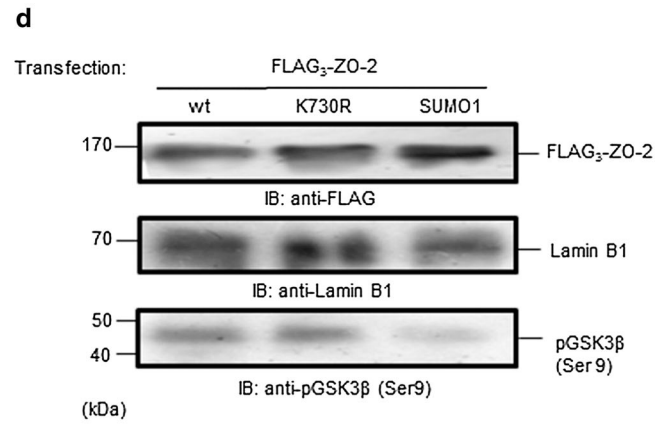
d
Transfection:
FLAG3-ZO-2
wt
K730R
SUMO1
170
FLAG3-ZO-2
IB: anti-FLAG
70
Lamin B1
IB: anti-Lamin B1
50
40
pGSK3β
(Ser 9)
IB: anti-pGSK3β (Ser9)
(kDa)

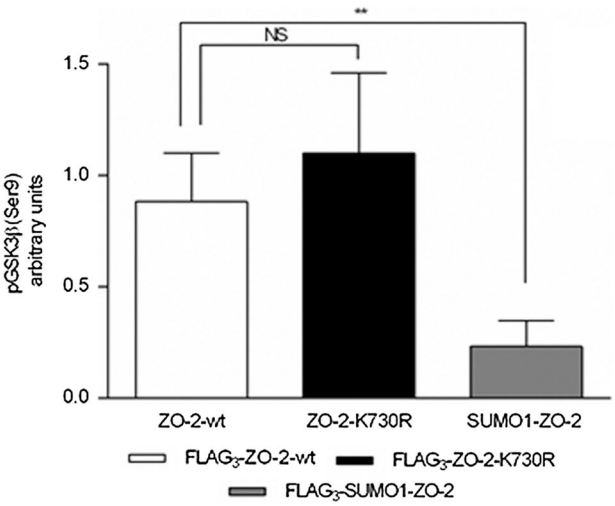
**
NS
1.5
1.0
0.5
0.0
pGSK3β(Ser9)
arbitrary units
ZO-2-wt
ZO-2-K730R
SUMO1-ZO-2
FLAG3-ZO-2-wt
FLAG3-ZO-2-K730R
FLAG3-SUMO1-ZO-2

◀**Fig. 7** ZO-2 interacts with GSK3β and decreases inhibitory phosphorylation of Ser9. **a** HEK-293 cells were transiently transfected with pCMV10 3xFLAG-ZO-2 and pCS2+GSK3β-myc$_6$ in the indicated combinations and immunoprecipitations were performed with an anti-myc antibody. Co-precipitating FLAG$_3$-ZO-2 was detected on Western blots with anti-FLAG M2 antibody. Lysate controls are shown in the *lower panels*. *, heavy chain of the precipitating antibody. **b** Endogenous protein complexes co-immunoprecipitated from MDCK cell lysates with the anti-ZO-2 antibody were analyzed by Western blotting with anti-GSK3β antibody. *PS*, pre-immune serum. **c** Proximity ligation assays (PLAs) indicate formation of endogenous ZO-2/GSK3β complexes in MDCKII cells. Non-target anti-P5D4 antibody was used as a control. – control using secondary antibodies alone. Z-stack projections of the confocal images are shown. Quantification of PLA signals of three independent experiments was done using the Fiji Software. The diagram on the *right* shows PLA signals related to cell number and normalized to the incubation with non-target antibody. Mean values ± SEM and significances analyzed by *t* test (*$p \leq 0.05$) are presented. *Scale bar* 50 µm. **d** MDCK cells were transfected with FLAG$_3$-ZO-2-wt, FLAG$_3$-ZO-2-K730R or FLAG$_3$-SUMO1ΔGG-ZO-2 and 24 h after transfection cells were lysed and analyzed by SDS-PAGE and Western blotting with anti-FLAG and anti-pGSK3β (Ser9) antibodies. Lamin B1 was used as a loading control. The *right panel* shows quantification of three independent experiments. **$p = 0.0085$ as assessed by one-way ANOVA followed by Bonferroni's post hoc test

The detection of endogenously SUMOylated proteins is often challenging since usually only minor fractions of the potential target proteins are SUMOylated and in addition the presence of SUMO proteases during lysis of cells results in rapid deconjugation [61]. To circumvent these problems we applied the UFDS (Ubc9 fusion-directed SUMOylation) system. In directly fusing the potential target with Ubc9 a more sensitive detection of the SUMO modification on a specific candidate target is possible [38]. Using this system a slower migrating species was detectable revealing that ZO-2 can be SUMOylated in cells. This band-shift was suppressed, when SENP1 was co-expressed but not with a protease-dead variant of SENP1 indicating that the shifted band indeed represents SUMO-modified ZO-2. When we included a mutated variant of SUMO2/3 that is less prone to deconjugation, the shifted band was stronger and a second shifted band appeared suggesting that ZO-2 can be multi- or poly-SUMOylated. Finally, PLAs provided further evidence for endogenous SUMOylated ZO-2 protein, which appeared to be predominantly located in the cytosol. Moreover, in vitro SUMOylation assays with an N-terminally deleted ZO-2 construct further confirmed that ZO-2 is a SUMOylation target (not shown).

Mutation of predicted potential SUMOylation sites in ZO-2 and subsequent UFDS assays identified K730 in human ZO-2 as a candidate SUMOylation site. Since the K730R mutation did not result in a complete abolishment of the shift band, it is probable that other sites in ZO-2

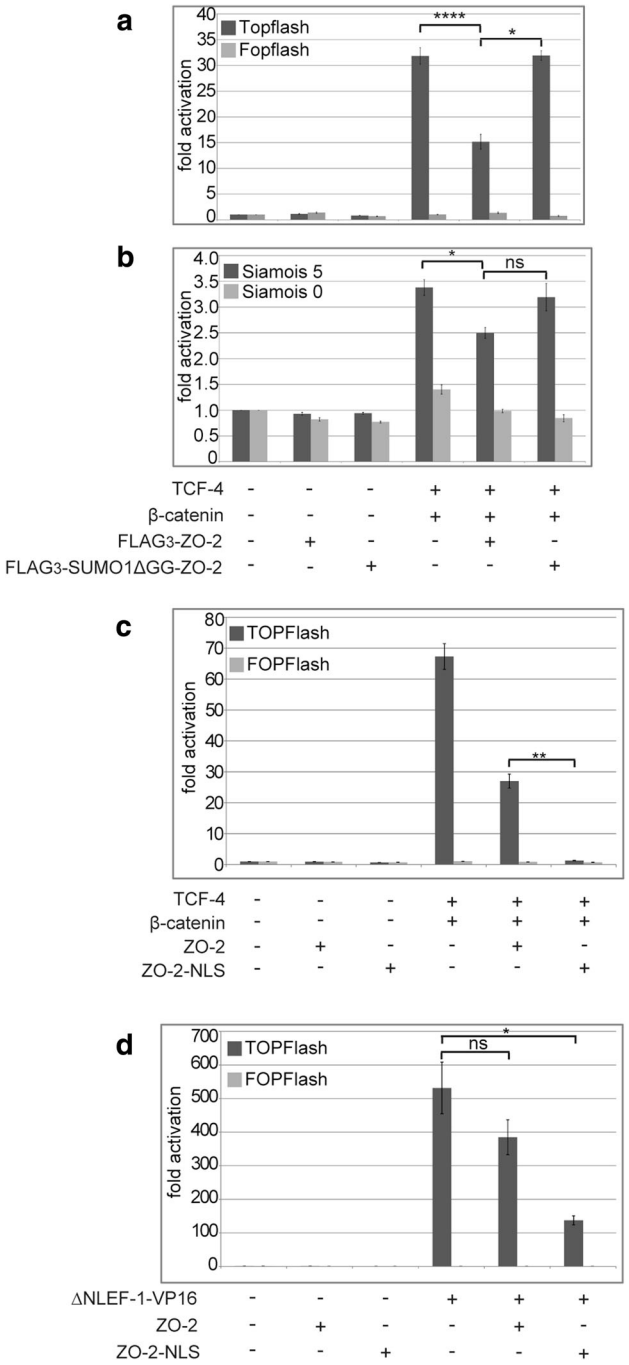

Fig. 8 SUMOylation impairs the repressive effect of ZO-2 on β-catenin signaling. **a**, **b** β-Catenin/TCF-4 transcriptional activity was measured in Topflash/Fopflash (**a**) or Siamois 5/0-Luc (**b**) reporter gene assays in HEK-293 cells transiently transfected with the indicated combinations of constructs. FLAG$_3$-tagged SUMO1ΔGG-ZO-2 was unable to repress β-catenin/TCF-4-mediated transcriptional activation in comparison to FLAG$_3$-tagged ZO-2-wt. **c** ZO-2-NLS efficiently represses β-catenin transcriptional activity in Topflash/Fopflash reporter gene assays. **d** Wild-type ZO-2 and ZO-2-NLS repress ΔNLEF-1-VP16-mediated transcription independently of β-catenin. Reporter gene assays represent at least three independent experiments. ****$p \leq 0.0001$; **$p \leq 0.01$; *$p \leq 0.05$; *ns* not significant

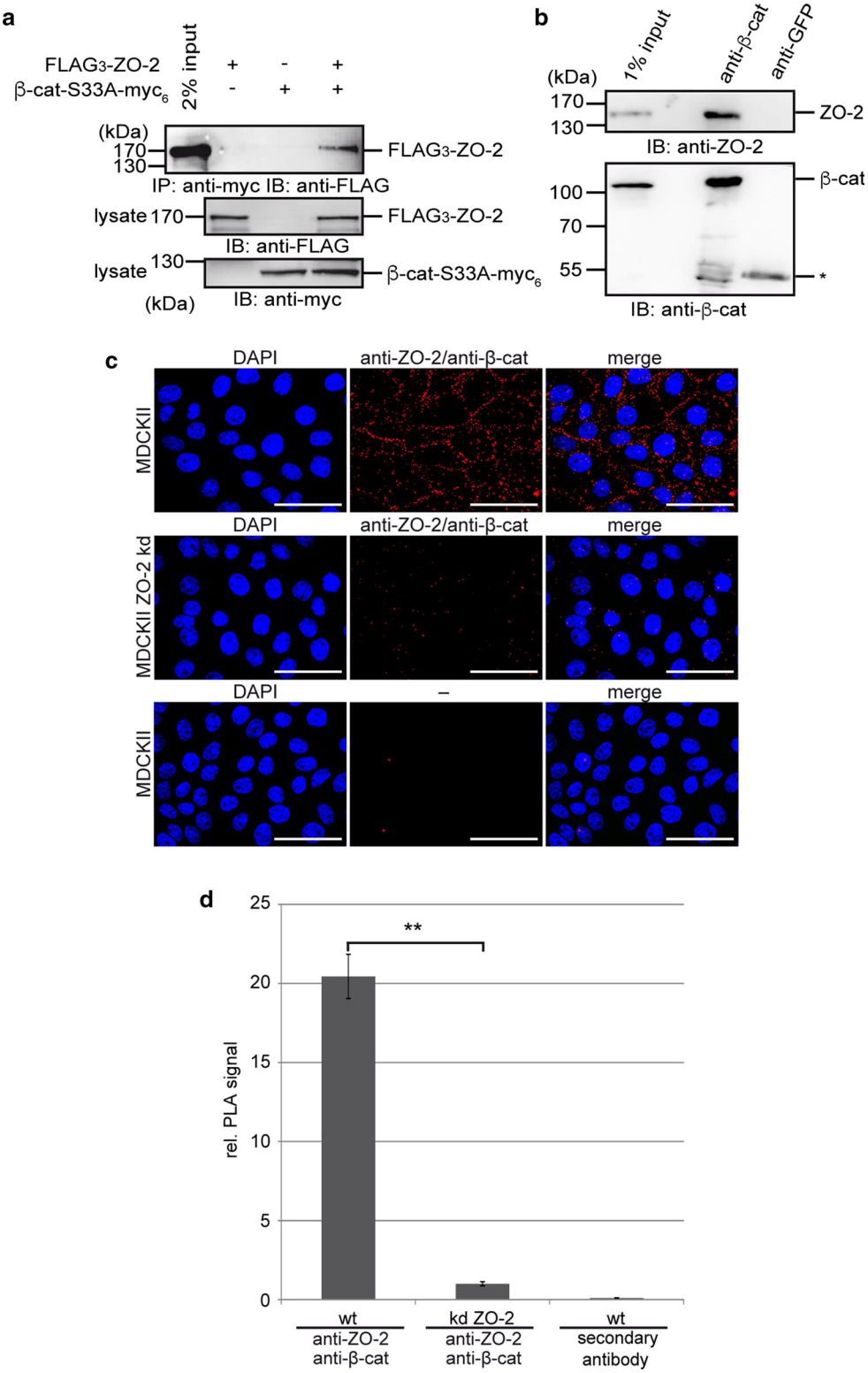

Fig. 9 ZO-2 forms a complex with β-catenin. **a** HEK-293 cells were transiently transfected with pCMV10 3xFLAG-ZO-2 and pCS2+-β-catenin-S33A-myc_6 in the indicated combinations and immunoprecipitations were performed with an anti-myc antibody. Co-precipitating $FLAG_3$-ZO-2 was detected on Western blots with anti-FLAG M2 antibody. The *lower panels* shows lysate controls. **b** Co-immunoprecipitation of endogenous ZO-2/β-catenin complexes with an anti-β-catenin antibody and detection of associated ZO-2 by western blotting. The *lower panel* shows precipitated β-catenin. Anti-GFP antibody was used as a non-targeting/negative control. *, heavy chain of the precipitating antibody. **c** Endogenous β-catenin forms a complex with ZO-2 in MDCKII cells as indicated by PLA. MDCKII ZO-2 knock-down cells were used as a control. – control using secondary antibodies alone. *Scale bar* 50 μm. **d** Quantification of PLA signals of three independent experiments using Fiji Software. $^{**}p \leq 0.01$

become SUMOylated when K730 is mutated. As the UFDS system artificially enhances SUMOylation it is very sensitive and may allow use of additional lysine residues for modification. It cannot be excluded that SUMOylation of these alternative residues is of no physiological relevance. A similar effect was also observed in studies with p53 SUMOylation mutants [38]. K730 is located in the GuK domain in close proximity to the NES-2 motif. This

allowed us to speculate that SUMOylation of K730 may affect nuclear export of ZO-2. To test this in more detail, fractionation experiments and nuclear recruitment assays were performed. Constitutive SUMOylation was mimicked by fusion of a protease-resistant SUMO1ΔGG to the ZO-2 N-terminus and compared with ZO-2-wt or ZO-2-K730R. These experiments confirmed previous observations that wild-type ZO-2 in proliferating cells first localizes to the nucleus and after export into the cytosol is integrated into TJs [25, 28]. The ZO-2-K730R mutant impaired in SUMOylation similarly is first detectable in the nucleus but then shows a massively reduced or delayed nuclear export suggesting that SUMOylation of ZO-2 is not important for nuclear entry but promotes nuclear export. The construct mimicking constitutive SUMOylated ZO-2 was not or only in minor amounts detectable in the nucleus in fractionation and nuclear recruitment assay, respectively, and predominantly localizes in the cytosolic/membrane fraction. We cannot finally exclude that the observed effects are caused by sterical or conformational changes induced by the SUMO-fusion. N-terminal $FLAG_3$- or HA-tags obviously do not affect the localization of the ZO-2 protein. Fusion of a SUMO-moiety to the ZO-2 C-terminus resulted in a wild-type-like behavior of ZO-2 in nuclear recruitment and reporter gene assays (not shown). However, we want to note that the $FLAG_3$-SUMO1ΔGG-ZO-2 construct was not impaired in binding to occludin in co-immunoprecipitation experiments suggesting that the conformation is not dramatically changed at least in this respect.

Our observations suggest that SUMOylation occurs in the cell nucleus and supports nuclear export of ZO-2. This finding is corroborated by the preferential cytosolic localization of endogenously SUMOylated ZO-2 observed in the PLAs. However, at the moment it is not known if integration into mature TJs requires a subsequent de-SUMOylation step. Previous studies identified sequence motives in the SH3-GuK-domain in ZO-1/ZO-2 as binding sites for occludin and α-catenin [62]. Since K730 of ZO-2 is located in this relevant region of the protein, SUMOylation is assumed to inhibit binding of ZO-2 to occludin. When we tested the SUMO-ZO-2 fusion protein in this respect, it was able to bind to occludin (not shown). However, this is not surprising, since the SH3-GUK-domain was not directly modified.

In future studies it will be interesting to see how SUMOylation of ZO-2 is coordinated with phosphorylation or O-GlcNAcylation events observed during ZO-2 trafficking [27, 28]. SUMOylation of K730 may induce conformational changes in ZO-2, which support nuclear export and enhance the interaction with the nuclear export machinery or inhibit nuclear import. A sequence of modification was reported to regulate the nuclear export of the tumor suppressor p53. A mono-ubiquitination by MDM2 induces a conformational change that is followed by a SUMOylation step by PIASy resulting in the formation of an export complex with CRM1 and p53 translocation into the cytoplasm [63]. Interestingly, SUMOylation may also be involved in the cell cycle-dependent nuclear export of ZO-2 during mitosis. Su et al. reported that Cdk1/cyclin B-dependent phosphorylation of Ubc9 enhances general SUMOylation activity [64]. This increase in SUMOylation activity may also lead to SUMOylation of ZO-2 and induce its nuclear export during mitosis [25]. Moreover, SUMOylation may affect the interaction of ZO-2 with TJ components which themselves are modified by numerous posttranslational modifications [44, 65].

In a last step we addressed if the SUMOylation-dependent localization of ZO-2 affects its signaling function. In this respect, we addressed the inhibitory activity of ZO-2 in the canonical Wnt signaling pathway. Consistent with its preferential nuclear localization, ZO-2-K730 is able to inhibit β-catenin/TCF-mediated transcriptional activation, whereas constitutively SUMOylated ZO-2 does not exhibit this repressive function. In this context we were interested in finding if ZO-2 can interact with β-catenin and this indeed was the case as shown by co-immunoprecipitation and pull-down experiments confirming a direct interaction. In line with this, PLAs provided further support that ZO-2 and β-catenin form common complexes. It is, however, noteworthy that PLA signals were predominantly detectable in the cell periphery. At the moment we only can speculate about the functional role of the ZO-2/β-catenin interaction. Similar to ZO-1, which also has been shown to co-precipitate with β-catenin [57], it can be speculated that β-catenin contributes to the transport of ZO-2 from the cytosol to newly forming TJs. However, other modes of action cannot be excluded. ZO-2 may directly or indirectly be involved in the regulation of β-catenin import/export into the nucleus, e.g. in analogy to the role of ZO-2 in the import of YAP2 [23].

Another step of regulation appears to occur at the level of GSK3β. Our previous studies have shown, that overexpression of ZO-2 reduces inhibitory phosphorylation of GSK3β on Ser9 [25]. In line with this observation, a genomic duplication of ZO-2 similarly results in a decreased phosphorylation of GSK3β [13]. In this context, here we showed that ZO-2 interacts with GSK3β in co-immunoprecipitation experiments. Again, PLAs provided evidence for common complexes of endogenous ZO-2 and GSK3β. Moreover, GSK3β directly binds to the ZO-2 N-terminal part in pull-down assays. This suggests that ZO-2 is a GSK3β target and GSK3β-dependent modifications are involved in modulation of ZO-2 function and localization. Interestingly, overexpression of the constitutively SUMOylated ZO-2

construct also induced a reduction of Ser9 phosphorylation in GSK3β. This should lead to an activation of its kinase activity and to enhanced β-catenin degradation. However, we observed a contrary effect suggesting that the repressive effect of ZO-2 on β-catenin-mediated transcription is indirect in line with the observation that ZO-2 also was able to repress ΔNLEF-1-VP16-mediated transcription independent of β-catenin. This also explains why we did not observe a consistent regulation of Wnt target genes in our previous study [25], where we observed a ZO-2-mediated downregulation of Axin-2 but not MMP-14. Moreover, it cannot be excluded that cytosolic SUMOylated ZO-2 binds β-catenin and directs it to cell–cell contacts consistent with complex formation of both proteins as detected in PLAs. Future studies have to further unravel the detailed mechanisms behind these observations.

Recently, we found that the lack of ZO-2 in MDCK cells increases the level of phosphorylation of Ser9 in GSK3β and β-catenin transcriptional activity [66]. This effect is the response to an increased activity of Akt due to an augmented cellular content of PIP_3. The latter occurs due to the inactivation of the Hippo pathway that promotes the nuclear accumulation of YAP and its transcriptional activity, which triggers the transcription of the gene for the catalytic subunit of PI3K [67], and miRNA-29 that inhibits the translation of PTEN [68].

The interaction of ZO-2 with GSK3β suggests that it is a GSK3β target. Multiple potential GSK3β phosphorylation sites can be found in the amino acid sequence of ZO-2 and GSK3β-dependent phosphorylation may modulate ZO-2 SUMOylation and activity. Moreover, it has been shown that GSK3β localization, activity and stability are regulated by SUMOylation. SUMOylation of GSK3β results in nuclear localization, and mutation of the SUMOylation site reduces kinase activity [69]. However, to our knowledge, it is not known how SUMOylation of GSK3β affects its activity in the Wnt-pathway.

Taken together, we conclude that SUMOylation of K730 represents a further posttranslational modification of human ZO-2 important for the regulation of its intracellular localization and signaling function.

Acknowledgments This work was supported by the Deutsche Forschungsgemeinschaft Research Group FOR 721 TP3 (HU 881/4-2) to OH and the Mexican National Council of Science and Technology to LGM (Conacyt, Grant 237241). Work done in the laboratory of OHK was supported by the Wilhelm Sander-Stiftung (#2010.078). Misael Cano received a Ph.D. scholarship from Conacyt No 283208. We acknowledge experimental support from Miguel Quirós. Human ZO-2 expression plasmid was kindly provided by Dr. Marius Sudol, Weis Center for Research, PA, USA. FLAG-SENP3 expression vectors were obtained from Dr. Stefan Müller, Max Planck Institute of Biochemistry, Martinsried, Germany and pSG5-His-SUMO1-Q94P/T65R was obtained from Dr. M. Lienhard Schmitz, Institute of Biochemistry, Medical Faculty, Justus-Liebig-University Giessen, Germany.

Compliance with ethical standards

Conflict of interest The authors declare no conflict of interest.

References

1. Van Itallie CM, Anderson JM (2014) Architecture of tight junctions and principles of molecular composition. Semin Cell Dev Biol 36:157–165
2. Gonzalez-Mariscal L, Tapia R, Chamorro D (2008) Crosstalk of tight junction components with signaling pathways. Biochim Biophys Acta 1778:729–756
3. Gonzalez-Mariscal L, Betanzos A, Nava P, Jaramillo BE (2003) Tight junction proteins. Prog Biophys Mol Biol 81:1–44
4. Gonzalez-Mariscal L, Dominguez-Calderon A, Raya-Sandino A, Ortega-Olvera JM, Vargas-Sierra O, Martinez-Revollar G (2014) Tight junctions and the regulation of gene expression. Semin Cell Dev Biol 36:213–223
5. Beatch M, Jesaitis LA, Gallin WJ, Goodenough DA, Stevenson BR (1996) The tight junction protein ZO-2 contains three PDZ (PSD-95/Discs-Large/ZO-1) domains and an alternatively spliced region. J Biol Chem 271:25723–25726
6. Bauer H, Zweimueller-Mayer J, Steinbacher P, Lametschwandtner A, Bauer HC (2010) The dual role of zonula occludens (ZO) proteins. J Biomed Biotechnol 2010:402593
7. Gonzalez-Mariscal L, Quiros M, Diaz-Coranguez M (2011) ZO proteins and redox-dependent processes. Antioxid Redox Signal 15:1235–1253
8. Traweger A, Toepfer S, Wagner RN, Zweimueller-Mayer J, Gehwolf R, Lehner C, Tempfer H, Krizbai I, Wilhelm I, Bauer HC, Bauer H (2013) Beyond cell-cell adhesion: emerging roles of the tight junction scaffold ZO-2. Tissue Barriers 1:e25039
9. Carlton VE, Harris BZ, Puffenberger EG, Batta AK, Knisely AS, Robinson DL, Strauss KA, Shneider BL, Lim WA, Salen G, Morton DH, Bull LN (2003) Complex inheritance of familial hypercholanemia with associated mutations in TJP2 and BAAT. Nat Genet 34:91–96
10. Sambrotta M, Strautnieks S, Papouli E, Rushton P, Clark BE, Parry DA, Logan CV, Newbury LJ, Kamath BM, Ling S, Grammatikopoulos T, Wagner BE, Magee JC, Sokol RJ, Mieli-Vergani G, University of Washington Center for Mendelian Group, Smith JD, Johnson CA, McClean P, Simpson MA, Knisely AS, Bull LN, Thompson RJ (2014) Mutations in TJP2 cause progressive cholestatic liver disease. Nat Genet 46:326–328
11. Sambrotta M, Thompson RJ (2015) Mutations in TJP2, encoding zona occludens 2, and liver disease. Tissue Barriers 3:e1026537
12. Kim MA, Kim YR, Sagong B, Cho HJ, Bae JW, Kim J, Lee J, Park HJ, Choi JY, Lee KY, Kim UK (2014) Genetic analysis of genes related to tight junction function in the Korean population with non-syndromic hearing loss. PLoS One 9:e95646
13. Walsh T, Pierce SB, Lenz DR, Brownstein Z, Dagan-Rosenfeld O, Shahin H, Roeb W, McCarthy S, Nord AS, Gordon CR, Ben-Neriah Z, Sebat J, Kanaan M, Lee MK, Frydman M, King MC, Avraham KB (2010) Genomic duplication and overexpression of TJP2/ZO-2 leads to altered expression of apoptosis genes in progressive nonsyndromic hearing loss DFNA51. Am J Hum Genet 87:101–109
14. Xu J, Kausalya PJ, Phua DCY, Ali SM, Hossein Z, Hunziker W (2008) Early embryonic lethality of mice lacking ZO-2, but not

ZO-3, reveals critical and nonredundant roles for individual zonula occludens proteins in mammalian development. Mol Cell Biol 28:1669–1678
15. Xu J, Anuar F, Ali MS, Ng MY, Phua DC, Hunziker W (2009) Zonula occludens-2 is critical for blood-testis barrier integrity and male fertility. Mol Biol Cell 20:4268–4277
16. Islas S, Vega J, Ponce L, Gonzalez-Mariscal L (2002) Nuclear localization of the tight junction protein ZO-2 in epithelial cells. Exp Cell Res 274:138–148
17. Betanzos A, Huerta M, Lopez-Bayghen E, Azuara E, Amerena J, Gonzalez-Mariscal L (2004) The tight junction protein ZO-2 associates with Jun, Fos and C/EBP transcription factors in epithelial cells. Exp Cell Res 292:51–66
18. Huerta M, Munoz R, Tapia R, Soto-Reyes E, Ramirez L, Recillas-Targa F, González-Mariscal L, Lopez-Bayghen E (2007) Cyclin D1 is transcriptionally down-regulated by ZO-2 via an E-box and the transcription factor c-Myc. Mol Biol Cell 18:4826–4836
19. Huang HY, Li R, Sun Q, Wang J, Zhou P, Han H, Zhang WH (2002) LIM protein KyoT2 interacts with human tight junction protein ZO-2-i3. Yi Chuan Xue Bao 29:953–958
20. Jaramillo BE, Ponce A, Moreno J, Betanzos A, Huerta M, Lopez-Bayghen E, Gonzalez-Mariscal L (2004) Characterization of the tight junction protein ZO-2 localized at the nucleus of epithelial cells. Exp Cell Res 297:247–258
21. Traweger A, Fuchs R, Krizbai IA, Weiger TM, Bauer HC, Bauer H (2003) The tight junction protein ZO-2 localizes to the nucleus and interacts with the heterogeneous nuclear ribonucleoprotein scaffold attachment factor-B. J Biol Chem 278:2692–2700
22. Mihlan S, Reiss C, Thalheimer P, Herterich S, Gaetzner S, Kremerskothen J, Pavenstadt HJ, Lewandrowski U, Sickmann A, Butt E (2013) Nuclear import of LASP-1 is regulated by phosphorylation and dynamic protein–protein interactions. Oncogene 32:2107–2113
23. Oka T, Remue E, Meerschaert K, Vanloo B, Boucherie C, Gfeller D, Bader GD, Sidhu SS, Vandekerckhove J, Gettemans J, Sudol M (2010) Functional complexes between YAP2 and ZO-2 are PDZ domain-dependent, and regulate YAP2 nuclear localization and signalling. Biochem J 432:461–472
24. Bautista-Garcia P, Reyes JL, Martin D, Namorado MC, Chavez-Munguia B, Soria-Castro E, Huber O, Gonzalez-Mariscal L (2013) Zona occludens-2 protects against podocyte dysfunction induced by ADR in mice. Am J Physiol Renal Physiol 304:F77–F87
25. Tapia R, Huerta M, Islas S, Avila-Flores A, Lopez-Bayghen E, Weiske J, Huber O, Gonzalez-Mariscal L (2009) ZO-2 inhibits cyclin D1 expression and cell proliferation and exhibits changes in localization along the cell cycle. Mol Biol Cell 20:1102–1117
26. Gonzalez-Mariscal L, Ponce A, Alarcon L, Jaramillo BE (2006) The tight junction protein ZO-2 has several functional nuclear export signals. Exp Cell Res 312:3323–3335
27. Chamorro D, Alarcon L, Ponce A, Tapia R, Gonzalez-Aguilar H, Robles-Flores M, Mejia-Castillo T, Segovia J, Bandala Y, Juaristi E, Gonzalez-Mariscal L (2009) Phosphorylation of zona occludens-2 by protein kinase Cε regulates its nuclear exportation. Mol Biol Cell 20:4120–4129
28. Quiros M, Alarcon L, Ponce A, Giannakouros T, Gonzalez-Mariscal L (2013) The intracellular fate of zonula occludens 2 is regulated by the phosphorylation of SR repeats and the phosphorylation/O-GlcNAcylation of S257. Mol Biol Cell 24:2528–2543
29. Geiss-Friedlander R, Melchior F (2007) Concepts in sumoylation: a decade on. Nat Rev Mol Cell Biol 8:947–956
30. Desterro JM, Rodriguez MS, Kemp GD, Hay RT (1999) Identification of the enzyme required for activation of the small ubiquitin-like protein SUMO-1. J Biol Chem 274:10618–10624
31. Johnson ES, Schwienhorst I, Dohmen RJ, Blobel G (1997) The ubiquitin-like protein Smt3p is activated for conjugation to other proteins by an Aos1p/Uba2p heterodimer. EMBO J 16:5509–5519
32. Desterro JM, Thomson J, Hay RT (1997) Ubch9 conjugates SUMO but not ubiquitin. FEBS Lett 417:297–300
33. Johnson ES, Blobel G (1997) Ubc9p is the conjugating enzyme for the ubiquitin-like protein Smt3p. J Biol Chem 272:26799–26802
34. Mukhopadhyay D, Dasso M (2007) Modification in reverse: the SUMO proteases. Trends Biochem Sci 32:286–295
35. Van Itallie CM, Mitic LL, Anderson JM (2012) SUMOylation of claudin-2. Ann N Y Acad Sci 1258:60–64
36. Westphal JK, Dörfel MJ, Krug SM, Cording JD, Piontek J, Blasig IE, Tauber R, Fromm M, Huber O (2010) Tricellulin forms homomeric and heteromeric tight junctional complexes. Cell Mol Life Sci 67:2057–2068
37. van Itallie CM, Fanning AS, Bridges A, Anderson JM (2009) ZO-1 stabilizes the tight junction solute barrier through coupling to the perijunctional cytoskeleton. Mol Biol Cell 20:3930–3940
38. Jakobs A, Koehnke J, Himstedt F, Funk M, Korn B, Gaestel M, Niedenthal R (2007) Ubc9 fusion-directed SUMOylation (UFDS): a method to analyze function of protein SUMOylation. Nat Methods 4:245–250
39. Haindl M, Harasim T, Eick D, Muller S (2008) The nucleolar SUMO-specific protease SENP3 reverses SUMO modification of nucleophosmin and is required for rRNA processing. EMBO Rep 9:273–279
40. Saul VV, Niedenthal R, Pich A, Weber F, Schmitz ML (2015) SUMO modification of TBK1 at the adaptor-binding C-terminal coiled-coil domain contributes to its antiviral activity. Biochim Biophys Acta 1853:136–143
41. Aberle H, Bauer A, Stappert J, Kispert A, Kemler R (1997) β-catenin is a target of the ubiquitin-proteasome pathway. EMBO J 16:3797–3804
42. Bauer A, Chauvet S, Huber O, Usseglio F, Rothbächer U, Aragnol D, Kemler R, Pradel J (2000) Pontin52 and Reptin52 function as antagonistic regulators of β-catenin signalling activity. EMBO J 19:6121–6130
43. Hämmerlein A, Weiske J, Huber O (2005) A second protein kinase CK1-mediated step negatively regulates Wnt signalling by disrupting the lymphocyte enhancer factor-1/β-catenin complex. Cell Mol Life Sci 62:606–618
44. Dörfel MJ, Westphal JK, Bellmann C, Krug SM, Cording J, Mittag S, Tauber R, Fromm M, Blasig IE, Huber O (2013) CK2-dependent phosphorylation of occludin regulates the interaction with ZO-proteins and tight junction integrity. Cell Commun Signal 11:40
45. Weiske J, Albring KF, Huber O (2007) The tumor suppressor Fhit acts as a repressor of β-catenin transcriptional activity. Proc Natl Acad Sci USA 104:20344–20349
46. Weiske J, Huber O (2005) The histidine triad protein Hint1 interacts with Pontin and Reptin and inhibits TCF-β-catenin-mediated transcription. J Cell Sci 118:3117–3129
47. Mittag S, Valenta T, Weiske J, Bloch L, Klingel S, Gradl D, Wetzel F, Chen Y, Petersen I, Basler K, Huber O (2016) A novel role for the tumour suppressor Nitrilase1 modulating the Wnt/β-catenin signalling pathway. Cell Discov 2:15039. doi:10.1038/celldisc.2015.1039
48. Ren J, Gao X, Jin C, Zhu M, Wang X, Shaw A, Wen L, Yao X, Xue Y (2009) Systematic study of protein sumoylation: development of a site-specific predictor of SUMOsp 2.0. Proteomics 9:3409–3412
49. Knipscheer P, Flotho A, Klug H, Olsen JV, van Dijk WJ, Fish A, Johnson ES, Mann M, Sixma TK, Pichler A (2008) Ubc9 sumoylation regulates SUMO target discrimination. Mol Cell 31:371–382

50. Mukherjee S, Thomas M, Dadgar N, Lieberman AP, Iniguez-Lluhi JA (2009) Small ubiquitin-like modifier (SUMO) modification of the androgen receptor attenuates polyglutamine-mediated aggregation. J Biol Chem 284:21296–21306
51. Cheng J, Wang D, Wang Z, Yeh ET (2004) SENP1 enhances androgen receptor-dependent transcription through desumoylation of histone deacetylase 1. Mol Cell Biol 24:6021–6028
52. Söderberg O, Gullberg M, Jarvius M, Ridderstrale K, Leuchowius KJ, Jarvius J, Wester K, Hydbring P, Bahram F, Larsson LG, Landegren U (2006) Direct observation of individual endogenous protein complexes in situ by proximity ligation. Nat Methods 3:995–1000
53. Pichler A, Melchior F (2002) Ubiquitin-related modifier SUMO1 and nucleocytoplasmic transport. Traffic 3:381–387
54. Kim JH, Choi HJ, Kim B, Kim MH, Lee JM, Kim IS, Lee MH, Choi SJ, Kim KI, Kim SI, Chung CH, Baek SH (2006) Roles of sumoylation of a reptin chromatin-remodelling complex in cancer metastasis. Nat Cell Biol 8:631–639
55. Kim JH, Lee JM, Nam HJ, Choi HJ, Yang JW, Lee JS, Kim MH, Kim SI, Chung CH, Kim KI, Baek SH (2007) SUMOylation of pontin chromatin-remodeling complex reveals a signal integration code in prostate cancer cells. Proc Natl Acad Sci USA 104:20793–20798
56. Aoki M, Hecht A, Kruse U, Kemler R, Vogt PK (1999) Nuclear endpoint of Wnt signaling: neoplastic transformation induced by transactivating lymphoid enhancing factor 1. Proc Natl Acad Sci USA 96:139–144
57. Rajasekaran AK, Hojo M, Huima T, Rodriguez-Boulan E (1996) Catenins and zonula occludens-1 form a complex during early stages in the assembly of tight junctions. J Cell Biol 132:451–463
58. Balda MS, Matter K (2008) Tight junctions and the regulation of gene expression. Biochim Biophys Acta 1788:761–767
59. Rodriguez MS, Dargemont C, Hay RT (2001) SUMO-1 conjugation in vivo requires both a consensus modification motif and nuclear targeting. J Biol Chem 276:12654–12659
60. Nishida T, Tanaka H, Yasuda H (2000) A novel mammalian Smt3-specific isopeptidase 1 (SMT3IP1) localized in the nucleolus at interphase. Eur J Biochem 267:6423–6427
61. Becker J, Barysch SV, Karaca S, Dittner C, Hsiao HH, Berriel Diaz M, Herzig S, Urlaub H, Melchior F (2013) Detecting endogenous SUMO targets in mammalian cells and tissues. Nat Struct Mol Biol 20:525–531
62. Müller SL, Portwich M, Schmidt A, Utepbergenov DI, Huber O, Blasig IE, Krause G (2005) The tight junction protein occludin and the adherens junction protein α-catenin share a common interaction mechanism with ZO-1. J Biol Chem 280:3747–3756
63. Carter S, Bischof O, Dejean A, Vousden KH (2007) C-terminal modifications regulate MDM2 dissociation and nuclear export of p53. Nat Cell Biol 9:428–435
64. Su YF, Yang T, Huang H, Liu LF, Hwang J (2012) Phosphorylation of Ubc9 by Cdk1 enhances SUMOylation activity. PLoS One 7:e34250
65. Dörfel MJ, Huber O (2012) Modulation of tight junction structure and function by kinases and phosphatases targeting occludin. J Biomed Biotechnol 2012:807356
66. Dominguez-Calderon A, Avila-Flores A, Ponce A, Lopez-Bayghen E, Calderon-Salinas JV, Luis Reyes J, Chavez-Munguia B, Segovia J, Angulo C, Ramirez L, Gallego-Gutierrez H, Alarcon L, Martin-Tapia D, Bautista-Garcia P, Gonzalez-Mariscal L (2016) ZO-2 silencing induces renal hypertrophy through a cell cycle mechanism and the activation of YAP and the mTOR pathway. Mol Biol Cell 27:1581–1595
67. Lin Z, Zhou P, von Gise A, Gu F, Ma Q, Chen J, Guo H, van Gorp PR, Wang DZ, Pu WT (2015) Pi3kcb links Hippo-YAP and PI3K-AKT signaling pathways to promote cardiomyocyte proliferation and survival. Circ Res 116:35–45
68. Tumaneng K, Schlegelmilch K, Russell RC, Yimlamai D, Basnet H, Mahadevan N, Fitamant J, Bardeesy N, Camargo FD, Guan KL (2012) YAP mediates crosstalk between the Hippo and PI(3)K-TOR pathways by suppressing PTEN via miR-29. Nat Cell Biol 14:1322–1329
69. Lee EJ, Hyun SH, Chun J, Shin SH, Yeon KH, Kwak MK, Park TY, Kang SS (2008) Regulation of glycogen synthase kinase 3β functions by modification of the small ubiquitin modifier. Open Biochem J 2:67–76